Age-related Changes in Auditory Cortex Without Detectable Peripheral Alterations: A Multi-level Study in Sprague–Dawley Rats

Florian Occelli, Florian Hasselmann, Julien Bourien, Michel Eybalin, Jean-Luc Puel, Nathalie Desvignes, Bernadette Wiszniowski, Jean-Marc Edeline, Boris Gourévitch

Age-related changes in auditory cortex without detectable peripheral alterations: a multi-level study in Sprague Dawley rats.

F. Occelli[1,2,a], F. Hasselmann[4,5], J. Bourien[4,5], M. Eybalin[4,5], J.L. Puel[4,5], N. Desvignes[1,2], B. Wiszniowski[1,2], J-M. Edeline[1,2,*], B. Gourévitch[1,2, b*]

Institut de NeuroScience Paris-Saclay (NeuroPSI), [1]UMR CNRS 9197, [2]University Paris-Sud, 91405 Orsay cedex, France;

Institute for Neurosciences of Montpellier, [3]INSERM - UMR 1051, [4]University of Montpellier, 34091 Montpellier cedex, France.

* The authors contributed equally

Correspondence should be addressed to
Jean-Marc Edeline
Paris-Saclay Institute of Neuroscience (Neuro-PSI)
UMR CNRS 9197
Université Paris-Sud, Bâtiment 446,
91405 Orsay cedex, France
E-mail: jean-marc.edeline@u-psud.fr
Phone: (+33) 1 69 15 49 72
Fax: (+33) 1 69 15 77 26

[a] Now at International Research Center for NeuroIntelligence (IRCN), University of Tokyo, Japan
[b] Now at Unité de Génétique et Physiologie de l'Audition, INSERM, Institut Pasteur, Sorbonne Université, F-75015 Paris, France.

Highlights :

- In female Sprague-Dawley, auditory periphery aged remarkably well: the auditory nerve threshold and the number of synapses between IHC and fibers were stable.
- Signs of aging of the central auditory system, albeit modest, were detectable in absence of peripheral alterations
- At the oldest tested age, behavioral performance was lower.
- Intrinsic, central aging effects can affect the perception of acoustic stimuli independently of the effects of aging on peripheral receptors

Number of Figures 10

Number of Tables 2 (plus one appendix)

Number of words for Abstract : 236

Number of words for Introduction : 754

Number of words for Discussion : 2251

Acknowledgments
This work was supported by grants from the French *Agence Nationale de la Recherche* (ANR) to B.G. (ANR-15-CE37-0007) and J-M.E. (ANR-14-CE30-0019), and from the "Attractivité" program of Paris-Sud University (2012). FH received support from the Hearing Prosthetist Group "Entendre" (R12090FF).
The authors are particularly grateful to Aurélie Bonilla, Fabien Lhericel, Joel Lefêvre and Céline Dubois for taking care of the rat colony. We thank two anonymous reviewers for their helpful comments.

Conflict of Interest

The authors declare no competing financial interests.

Abstract

Aging is often considered to affect both the peripheral (i.e. the cochlea) and central (brainstem and thalamus-cortex) auditory systems. We investigated the effects of aging on the cochlea, brainstem and cortex of female Sprague Dawley rats. The auditory nerve threshold remained stable between the ages of 9 and 21 months, as did distortion product otoacoustic emissions and the number of ribbon synapses between inner hair cells and nerve fibers. The first clear signs of aging appeared in the brainstem, in which response amplitude decreased, with thresholds remaining stable until the age of 15 months, and increasing slightly thereafter. The responses of primary auditory cortex neurons revealed specific effects of aging: at 21 months, receptive fields were spectrally narrower and the temporal reliability of responses to communication sounds was lower. However, aging had a null or even positive effect on neuronal responses in the presence of background noise, responses to amplitude-modulated sounds, and responses in gap-detection protocols. Overall, inter-animal variability remained high relative to the variability across groups of different ages, for all parameters tested. Behavioral performance for AM noise modulation depth detection was worse in 21-month-old animals than in other animals. Age-related alterations of cortical and behavioral responses were thus observed in animals displaying no signs of aging at the peripheral level. These results suggest that intrinsic, central aging effects can affect the perception of acoustic stimuli independently of the effects of aging on peripheral receptors.

Keywords: central auditory system, synaptic ribbons, behavioral task, multi-unit recordings, compound action potential

Introduction

In humans, age-related hearing loss (ARHL), also known as presbycusis, is highly prevalent (35-50% of people >65 years old; (Parham et al., 2011)). In addition to repeated exposure to loud noises, genetic factors, lifestyle and medical history modulate the occurrence and extent of ARHL (Helzner et al., 2005). The increasing life expectancy of the human population has rendered the effects of aging more prominent, and it is crucial to improve our understanding of presbycusis, which decreases quality of life and is associated with depression, anxiety and social isolation (Ciorba et al., 2012).

Many psychoacoustic studies in humans have described age-related hearing loss (Schuknecht, 1955; Schuknecht and Kirchner, 1974; Pearlman, 1982; Humes et al., 2012). Threshold elevations are reported on audiograms (Gates and Mills, 2005), and the other deficits observed are: (i) a decline in the ability to discriminate between close frequencies (Clinard et al., 2010) (ii) a degradation of gap detection in sounds (Harris et al., 2010) and (iii) an impairment of the ability to understand speech in noisy environments (Frisina and Frisina, 1997). Animal studies have described effects of aging on the cochlea, the auditory nerve and the lower levels of the auditory system. An initial massive loss of outer hair cells, together with a much less severe and more variable loss of inner hair cells, has been described (Tarnowski et al., 1991). Together with a loss of auditory nerve fibers (Schmiedt et al., 1996), those alterations logically lead to the increases in threshold reported in quantifications of auditory brainstem responses (Gratton et al., 2008) and the decrease in frequency selectivity of the auditory nerve fibers (Hellstrom and Schmiedt, 1996). Surprisingly, few studies have described the effects of aging in the upper levels of the auditory system, including the primary auditory cortex (AI). The receptive fields were found to be abnormal in aged (30 months old) Fisher 344 rats (Turner et al., 2005). Aged primates with normal audiograms have been

reported to lack the sharpening of spatial tuning normally observed in younger animals (Juarez-Salinas et al., 2010). These monkeys had stronger cortical evoked responses, particularly for onset responses (Engle and Recanzone, 2012). By contrast, in three-year-old guinea pigs with a hearing loss of about 30 dB, the receptive fields displayed weaker and longer duration responses, higher thresholds and narrower bandwidths (Gourévitch and Edeline, 2011). Most biochemical studies of the cortex have reported changes to GABAergic neurotransmission (reviewed in (Caspary et al., 2008)). For example, Ling and colleagues (Ling et al., 2005) reported that levels of GAD_{67} protein were lower in old rats (20-30 months of age) than in young rats. All these alterations follow a particular timing, which differs from strain to strain.

We describe here the impact of aging on anatomical and physiological measurements derived from the cochlea (distortion product otoacoustic emissions, DPOAE; ribbon synapse counting), the auditory nerve (compound action potential, CAP), the brainstem (ABR) and AI in female Sprague Dawley (SD) rats aged 9, 15 and 21 months. On average, the mean life span of normal female Sprague Dawley rats was found to be either 760 days (Davis et al., 1956) or 680 days (excluding tumor-related deaths) (Durbin et al., 1966), which means that our oldest animals were roughly between 80% and 90% of their average lifespan. Sprague Dawley rats experience an age-related hearing threshold shift between 20dB and 30dB starting after 18 months of age (Stenqvist, 2000; Sanz-Fernández et al., 2015; Costa et al., 2016) and, up to now, the aging of their central auditory system has not been documented. In addition to bandwidth and threshold of tuning curves of AI neurons, we quantified neuronal responses to gaps and various depths and rates of amplitude modulation. We also quantified the responses to natural communication sounds presented with (and without) different levels of background broadband white noise. We evaluated the behavioral consequences of the age-induced alterations to the auditory system, through a task in which rats were required to

discriminate between different depths of amplitude-modulated noise. Finally, we tried to identify one of the neurobiological substrates of potential deficits, by estimating the number of GABAergic neurons in the primary auditory cortex. Thus, unlike previous studies, we investigated each animal from the most peripheral (DPOAE) to the most central (AI) level, with electrophysiological, immunohistochemical and behavioral techniques. We found that age-related alterations emerged within the cortex independently of peripheral alterations, consistent with the notion of specific "central aging". Moreover, our results suggest that both peripheral and central aging may be very limited in the auditory system of female Sprague Dawley rats.

Materials and Methods

Subjects

Recordings were obtained from the primary auditory cortex of adult female Sprague Dawley rats. The animals were obtained from Janvier Laboratories at an age of two months, and were housed for 6, 12 or 18 months in a facility with controlled humidity (50-55%) and temperature (22-24° C) conditions, under a 12 h light/12 h dark cycle (lights on at 7:30 a.m..) with free access to food and water. At the end of experiments, animals were 9, 15, 21 months. A total of 10 animals were initially used in the group 9 months, 10 others in the group 15 months and 20 in the group 21 months. Given the well-documented susceptibility of female Sprague Dawley rats to mammary tumors (Davis et al., 1956; Freedman et al., 1990; Fay et al., 1997; Jowa and Howd, 2011), all aged animals were regularly examined by the staff from the animal facility, and any found to have tumors were excluded from the study. The protocol was approved by the local ethics committee (Paris-Sud University, CEEA No. 59, project 2014-25) and used the procedures 32-2011 and 34-2012 of this committee. Each animal was subjected to the following protocols, in the following order, as described below: the behavioral task for three weeks; extracellular recordings in the primary auditory cortex; two weeks of rest; functional peripheral assessments; immunohistochemistry. The final sample sizes for the various groups of animals are summarized in Table 1 and are as follows: 9 to 12 animals per group participated to the behavior, 8 to 9 to the recordings in AI, 5 to 9 to the DPOAE/CAP recordings and 4 to 6 to the immunochemistry study.

Behavioral task

After two sessions of familiarization (lasting 5 min each) with the test apparatus, rats were trained to discriminate between an amplitude-modulated white noise (4 Hz, 100% depth

modulation; CS+) and an unmodulated white noise (CS-) in a two-compartment shuttle box. Both stimuli lasted 5 s and they were presented a mean of 30 s apart (range: 20 s -75 s). The rat was required to change compartment on CS+ presentation. A lack of response to the CS+ stimulus triggered a 0.3 mA footshock lasting 10 s, which was stopped immediately if the rat switched compartment. On presentation of the CS- signal, no change in compartment was required. The CS+ and CS- stimuli were presented 40 times per session. The time taken to switch compartments after the onset of the CS+ signal was also recorded.

Performance was estimated by calculating the A' index (Verde et al., 2006), which is a non-parametric analog of *d'* and quantifies the discrimination between two stimuli, as follows:

$$A' = \frac{1}{2} + \frac{(H-F)(1+H-F)}{4H(1-F)} \text{ if } H \geq F$$

and

$$A' = \frac{1}{2} + \frac{(F-H)(1+F-H)}{4F(1-H)} \text{ if } H < F$$

where H is the hit rate (the proportion of switches on CS+ presentation) and F is false alarm rate (the proportion of switches on CS- presentation). When $H=F$ (same number of responses to the CS+ and CS- stimuli in the 40 trials) then $A'=0.5$. When $H=1$ and $F=0$ then $A'=1$. In our experiment, a successful session was defined as a session where $H \geq 0.5$ and $A' \geq 0.75$.

During the first 10 sessions, each rat was required to complete three sessions in a row successfully, otherwise the training was stopped. Once the animal had reached this level of performance, the second phase of the task began, in which we determined the smallest modulation depth for which the rat discriminated between CS+ and CS-. Each session was split into two parts: an initial "recall phase" during which the animal had to discriminate between 0% vs. 100% modulated white noise for 20 random presentations, followed by a test phase during which the animal had to discriminate between 0% and a particular modulation depth, 80%, 60%, 40% or 20%. Only one value of modulation depth was used in this second

part of the session, the highest modulation depth for which the animal did not perform well at the previous session. The animal had a maximum of three sessions to perform successfully at a given modulation depth before a lower modulation depth was selected. If the animal satisfied this criterion, a lower modulation depth was tested at the next session. If the animal did not satisfy the criterion after three sessions, or it satisfied this criterion only at the lowest modulation depth (20%), training was stopped.

Extracellular recordings in the primary auditory cortex

Acoustic stimuli

Acoustic stimuli were generated in Matlab, transferred to an RP2.1-based sound delivery system (TDT) and sent to a Fostex speaker (FE87E). The speaker was placed 2 cm away from the right ear of the rat. At this distance, the speaker produced a flat spectrum (± 3 dB) between 140 Hz and 36 kHz after calibration. The speaker was calibrated with a Brüel & Kjaer (B&K) 4133 microphone, also placed 2 cm away from the speaker and coupled to a B&K 2169 preamplifier and a Marantz PMD671 digital recorder. The transfer function of the speaker was estimated with noise and pure tones, then inverted and fitted with a sixth-order IIR filter. This filter was applied to all sounds sent to the speaker. Spectrotemporal receptive fields (STRFs) were determined with 97 gamma-tone frequencies (the product of a gamma distribution and sinusoidal tone, (Lyon et al., 2010)), covering eight octaves (0.14-36 kHz), presented in a random order at a rate of 4.15 Hz and at 75 dB SPL. The frequency response area (FRA) was determined with the same set of tones presented from 75 to 5 dB SPL (5 dB steps, random order) at a rate of 2 Hz. Each tone was presented eight times at each intensity.

The responses to a set of natural stimuli were tested. We first tested responses to heterospecific guinea pig vocalizations, corresponding to three representative examples of a whistle call used in a previous study (Gaucher et al., 2013), concatenated into a one-second stimulus presented 25 times. We also used a one-second snatch of bird song from this

previous study. The vocalizations were presented with and without various levels of white noise (60, 65 and 70 dB SPL). We did not use rat vocalizations here, because pilot studies reported that the typical 22 kHz alarm call (Portfors, 2007; Brudzynski, 2009) had a limited spectral content and actually evoked poor responses of little use for auditory cortex neuron characterization. We then used a gap detection protocol, involving a 300 ms guinea pig whistle (the first call from the set of three used above), split into two halves separated by a gap of 2, 4, 8, 16, 32 or 64 ms of silence. A 1 ms ramp was used as the transition between vocalization and the silent gap, on both sides of the gap. We used 25 repetitions of the stimulus for each of the six gap values.

Responses to amplitude-modulated white noise were tested with 15 presentations of 100% modulated white noise, at 2 Hz to 50 Hz. Responses to modulation depth were assessed with 20 presentations of one second of white noise at 4 Hz, with a modulation depth ranging from 0% to 100%.

Surgical procedure

The animal received an initial dose of ketamine and xylazine (100mg/kg i.p. and 15mg/kg i.p. respectively) supplemented by lower doses of ketamine (20 mg/kg) and xylazine (4 mg/kg) until reflex movements were no longer observed when the hind paw was pinched. Liberal amounts of a local anesthetic (2% xylocaine) were injected subcutaneously into the skin above the skull and the temporal muscles. The animal was placed in a stereotaxic frame, a craniotomy was performed above the left temporal cortex, and the temporal bone was placed in sterile saline. The opening was 9 mm wide and began at the point of intersection between the parietal and temporal bones, at a height of 5 mm (Manunta and Edeline, 1997, 1998, 2004). The dura above the auditory cortex was carefully removed under binocular control without damaging the blood vessels. At the end of surgery, a pedestal was created with dental

acrylic cement, to make it possible to fix the animal's head in place without trauma during the recording session. The stereotaxic frame supporting the animal was placed in a sound-attenuating chamber (IAC, model AC1).

Recording procedure

Data were collected from multiunit recordings in the primary auditory cortex (area AI). Extracellular recordings were obtained from arrays of 16 tungsten electrodes (ø: 33 µm, <1 MΩ) composed of two rows of eight electrodes separated by 1000 µm (350 µm between electrodes of the same row). A silver wire, used as the ground electrode, was inserted between the temporal bone and the dura matter on the contralateral side. The estimated location of AI was 4-7 mm posterior to bregma and 3 mm ventral to the superior suture of the temporal bone (corresponding to area AI as defined by (Paxinos and Watson, 2005). The raw signal was amplified by a factor of 10,000 (TDT Medusa) and processed by a multichannel data acquisition system (TDT RX5). The signal collected from each electrode was filtered (610-10,000 Hz) to extract multi-unit activity (MUA). The trigger level was carefully set for each electrode so as to select the largest action potentials from the signal. Online and offline examinations of the waveforms suggested that the MUA collected here consisted of action potentials generated by three to six neurons close to the electrode. At the beginning of each recording session, we set the position of the electrode array such that the two rows of eight electrodes could sample neurons responding from low to high frequencies in the rostro-caudal direction.

Recording session

The insertion of an array of 16 electrodes into the cortical tissue almost systematically induced a deformation of the cortex. The cortex was allowed to return to its initial shape over

a recovery period of at least a 30 minutes, and the array was then slowly lowered. STRFs were used to assess the quality of our recordings and to adjust electrode depth. The recording depth was 300-700 µm, corresponding to layer III/IV and the upper part of layer V, according to Roger and Arnault (Roger and Arnault, 1989). Once clear tuning was obtained for at least 12 of the 16 electrodes, and the stability of the recordings was satisfactory, the protocol was initiated, with the presentation of acoustic stimuli in the following order: gamma-tones to determine the STRF (5 min), followed by the FRA (12 min), followed by the different sets of vocalizations at 75 dB SPL without noise (3 min) and with increasing noise levels (60, 65 and 70 dB SPL, 3 min each). The gap detection protocol was then performed (3 min), followed by 3 min of spontaneous activity, and then depth-modulated noise at 75 dB SPL (4 min), amplitude-modulated noise at 75 dB SPL (7 min) and a final period of three minutes of constant white noise at 75 dB SPL. The presentation of this entire series of stimuli lasted 49 minutes. This set of stimuli was used with the electrode array positioned at two to five locations per animal, in the primary auditory cortex.

Quantification of responses to pure tones

The STRFs derived from MUA were obtained by constructing post-stimulus time histograms (PSTHs) for each frequency, with 1 ms time bins. All spikes falling in the averaging time window (starting at stimulus onset and lasting 100 ms) were counted. Thus, STRFs are matrices of 100 abscissa (time) bins multiplied by 97 ordinates (frequency) bins. All STRFs were smoothed with a uniform 5x5 bin window.

For each STRF, at a given intensity, the best frequency (BF) was defined as the frequency at which the highest firing rate was recorded. At each intensity, peaks of significant response were automatically identified as follows: A positive peak in the MU-based STRF was defined as a firing rate contour above the mean level of baseline activity (estimated from

the first 10 milliseconds of STRFs at all intensities) plus six times the standard deviation of the baseline activity. For a given site and a given intensity, three measurements were extracted from the peaks: "total bandwidth", defined as the sum of all peak widths in octaves; the latency of the first spike of the significant peaks (the time taken to reach this spike); and "response duration", the time interval between the first and last spikes of the significant peaks.

Responses to vocalizations

Many previous studies have stressed that the temporal spike patterns of the neuronal discharges observed when communication sounds are presented are crucial for the discrimination performance of cortical neurons (Schnupp et al., 2006; Engineer et al., 2008; Huetz et al., 2009; Shetake et al., 2011). We quantified the between-trial reliability of neuronal responses to vocalizations, by calculating the spike-timing reliability coefficient (*CorrCoef*). This index corresponds to the normalized covariance between each pair of action potential trains recorded on the presentation of a given vocalization and was calculated as follows:

$$CorrCoef = \frac{1}{N(N-1)} \sum_{i=1}^{N-1} \sum_{j=i+1}^{N} \frac{\sigma x_i x_j}{\sigma x_i \sigma x_j}$$

where N is the number of trials and $\sigma x_i x_j$ is the normalized covariance for a time lag of 0 between spike trains x_i and $x_{j,}$ where i and j are the trial numbers. Spike trains x_i and x_j were previously convolved with a 10 ms-wide Gaussian window. This value of temporal precision was chosen because it maximized mutual information (Huetz et al., 2009). It was shown that the *CorrCoef* was not influenced by fluctuations of firing rate (Gaucher et al., 2013). These simulations also made it possible to calculate the probability of the *CorrCoef* value: 0.026 for a 0.01 confidence interval (Gaucher et al., 2013).

Gap detection analysis

We first constructed post-stimulus time histograms (PSTHs) of the responses to the vocalizations including a gap with a 2 ms time bin and a 5 ms uniform smoothing window. We considered the neural response to be modulated by the presence of the gap if an onset peak appeared in the PSTH, typically at the beginning of the second half of the vocalization, immediately after the gap. The peak was considered significant if its maximum amplitude was above the mean + 4 STD of the PSTH values over a time interval of 50 ms immediately before the gap. We chose a gap-in-vocalization rather than a gap-in-noise sound for several reasons: this is a more realistic sound than a noise, the vocalization induced very strong evoked responses in our neurons population, the vocalization was broadband and finally its spectral content was stationary in time at the gap location, avoiding any across-channel gap detection.

Analyses of temporal tMTF and depth-MTF.

We first constructed PSTHs for each amplitude- or depth-modulated sound, with a 5 ms time bin. For each modulation frequency or depth modulation, we then calculated vector strength (VS), defined by (Goldberg and Brown, 1969) as a measurement of the degree of phase-locking (or synchronization) of the spikes with the stimulus envelope. The VS is a coefficient that varies between 0 and 1.

End of the recording session

After three to six hours of recording, the skull covering the temporal bone was carefully placed back over the auditory cortex and secured in place with a very thin layer of dental cement. The skin was cleaned and sutured to close the wound and an analgesic

(buprenorphine, 0.05 mg/kg, s.c.) and an antibiotic (Convenia, 0.8 mg/kg, s.c.) were injected into the animal. The animal's health was monitored every six hours for 24 h, and the animal was kept in a separate cage for a few days before being returned to the colony room. After two to three weeks of recovery, the animals were sent to the INM (Montpellier) via a specialist transporter (Sanitrans, France), for peripheral assessment.

Peripheral assessments (DPOAEs, CAPs, ABRs)

Distortion product otoacoustic emissions (DPOAEs)

DPOAEs were used as a measure of the functional integrity of outer hair cells. DPOAEs were collected under anesthesia (a mixture of Zoletil 50 (tiletamine, 40 mg/kg) and Rompun (xylazine, 3 mg/kg)). They were recorded in the external auditory canal with an ER-10C S/N 2525 probe (Etymotic Research Inc. Elk Grove Village, IL, USA) consisting of two emitters and one microphone. The two primary tones were generated, and the distortion was processed by the Cubdis HID 40133DP system (Mimosa Acoustics, Champaign, IL, USA). The two tones were presented simultaneously, with f_2 sweeping from 0.5 kHz to 16 kHz in quarter-octave steps, and maintenance of the f_2/f_1 ratio constant at 1.2. The primary intensities of f_2 and f_1 were set at 60 and 55 dB SPL, respectively. For each frequency, the cubic distortion product $2f_1$-f_2 and the neighboring noise magnitudes were measured and expressed as a function of f_2.

Functional hearing assessments (ABR and CAP)

These recordings were also carried out under anesthesia (Zoletil 50 (tiletamine, 40 mg/kg) and Rompun (xylazine, 3 mg/kg)) in a Faraday-shielded anechoic sound-proof cage. Rectal temperature was measured with a thermistor probe, and maintained at 38°C ± 1°C with a heated blanket placed underneath the animal. Signals were generated, acquired and

processed with an NI PXI-4461 signal generator (National Instruments) controlled with LabVIEW software. Bursts of pure tones (1 ms rise/fall, 10 ms duration, 11 bursts/s, 500 or 200 presentations per level for ABRs and CAP, respectively, alternating polarity) were delivered by a JBL 075 loudspeaker (James B. Lansing Sound) positioned 10 cm away from the ear tested, in calibrated free-field conditions. Electrophysiological signals (×20,000) were amplified with a Grass P511 differential amplifier with a 300 Hz to 3.5 kHz bandpass.

ABRs were recorded from three subcutaneous needle electrodes placed on the vertex (active), near the bulla of the tested ear, and in the neck muscles (ground). The CAP of the auditory nerve was recorded from an electrode located in the round window niche (active) and two subcutaneous needle electrodes placed on the pinna of the ear tested and in the neck muscles (ground). Intensity-amplitude functions were obtained for ABRs and CAPs, at each frequency tested (1, 2, 4, 8, 16, 24, 32 kHz), by varying the intensity of the tone burst from 0 to 80 dB SPL, in 5 dB increments. The ABR threshold was defined as the minimum sound intensity required to elicit a well-defined and reproducible wave II from the cochlear nucleus (Chen and Chen, 1991). CAP amplitude was measured between N1 and P1, with CAP threshold defined as the dB SPL required to elicit a measurable response of greater magnitude than the noise level.

Immunohistochemistry

Quantification of GAD67 labeling

GAD67 labeling was studied as a measure of possible changes in GABAergic inhibition. To this aim, at the end of the CAP recording session, the rats were deeply anesthetized with a mixture of ketamine and xylazine (200 mg/kg body weight and 15 mg/kg, respectively, i.p.) and transcardially perfused with 150 ml of saline and 1,000 ml of a fixative solution consisting of 4% paraformaldehyde (PFA) in 0.1 M phosphate buffer (pH 7.4). The

brains were collected and fixed in 4% PFA; they were then incubated in incremental concentrations of sucrose (10, 20 and 30%). Each brain was sliced (40 µm sections) on a cryostat (HM55O, Microm, Thermo Scientific), from stereotaxic coordinates -4 mm to -6 mm relative to bregma (Paxinos and Watson 2009, 6th edition). One in every four slices was stained with Nissl stain and three co-authors (JME, FO, ND) examined the stained coronal sections to select the anterior-posterior level corresponding to the center of AI. One adjacent section (immediately before or after the Nissl-stained slice) was used for GAD67 labeling. The brain slices were rinsed in 1 x PBS and endogenous peroxidases were inactivated by incubation in 1 x PBS supplemented with 10% methanol and 10% H_2O_2. The coronal sections were then washed and permeabilized in 2.5% Triton in 1 x PBS (PBST). Nonspecific antigen sites were blocked by incubation with 5% normal goat serum and 1% BSA in PBST. The sections were then incubated overnight at 4°C with the primary anti-GAD67 antibody (Euromedex, GeneTex) diluted 1:500 in the same blocking solution. The sections were washed in PBST then incubated with a secondary antibody (biotinylated anti-rabbit IgG antibody, EuroBio) for two hours at room temperature. Staining was detected with an ABC kit (EuroBio), in accordance with the manufacturer's instructions. Sections were then mounted on glass slides (Fisher) in 0.3% PB gelatin. On the third day, slides were dehydrated and mounted in Eukitt (Fisher). Photomicrographs were taken with an upright optical microscope (Olympus microscope, BX60) equipped with mapping software (MercatorPro; ExploraNova, France). Immunolabeling was assessed in two predefined areas (800x300 µm) manually delimited in the center of AI, in the supragranular and infragranular layers. The immunolabeled cells were counted by an experimenter blind to the age of the animal.

Number of ribbon synapses per inner hair cell along the tonotopic axis

The immunohistochemical method for assessing the number of synapses per inner hair cell (IHC) has been described in detail elsewhere (Bourien et al., 2014; Batrel et al., 2017). Briefly, the presynaptic IHC ribbons were identified with a mouse anti-CtBP2 antibody (1:500; BD Biosciences, San Diego, CA). Glutamate receptors were labeled with a mouse antibody raised against the C-terminus of the GluA2 subunit, IgG2a (1:200, Millipore, Billerica, MA). A 3D, custom algorithm was used to detect the juxtaposition of pre- and post-synaptic structures in stacked confocal images. Once the ribbons had been counted, the corresponding coding frequency of each ribbon was inferred from the rat cochlear place frequency map (Müller, 1991). A second-order polynomial was then fitted to synapse count as a function of position relative to the cochlea apex (Meyer et al., 2009).

Statistical analysis

We mainly used ANOVA tests (one-way, two-way, three-way) to look for effects in our data, followed by post-hoc unpaired t-tests with Bonferroni correction. We tested for and found normal distributions of residuals (using QQ plots) and equal variances (Levene's test, Levene, 1960) in the great majority of our sampled distributions. Deviations from normality, when found, were moderate. Robustness of ANOVA tests to such deviations (Lix et al., 1996; Blanca et al., 2017) as well as the large sample size in our groups (see Table 2) confirm ANOVA as a valid option, in addition to the fact that no satisfying non parametric solution currently exists for two-way and three-way tests.

Results

The results presented below were obtained from three groups of adult female Sprague Dawley rats aged 9 (n=10), 15 (n=9) and 21 (n=12; see Table 1) months raised in a standardized animal facility with *ad libitum* access to food and water. The sample sizes for the various groups of animals are summarized in Table 1. Once an animal reached the age for testing, it underwent behavioral training for three weeks. For each animal, we obtained cortical recordings under ketamine/xylazine anesthesia 24 to 48 hours after the last training session; between 431 and 297 neuronal recordings were collected from AI. The compound action potential (CAP) of the auditory nerve, the auditory brainstem responses (ABRs) and the distortion products of the acoustic emissions (DPOAEs) were collected in a separate session under tiletamine/xylazine anesthesia. Functional quantifications, such as the determination of auditory thresholds, were thus possible in the periphery, brainstem and cortex of the same animal, as illustrated in Figure 1. The data for this animal highlight the similarity of the thresholds at the peripheral, brainstem and cortical level, except around 16 kHz. The brain of the animal was then collected for immunolabeling. For the sake of readability, only the *p* values (each indexed by a letter) are reported in the text; the details of each statistical test are provided in appendix.

Cochlear evaluations

For the DPOAEs obtained from rats aged 9, 15 and 21 months (Figure 2A), over the whole frequency range above the noise level (3-16 kHz, noise represented by the gray line), the amplitudes of the distortion products were similar for all three groups of animals (age effect p^a=0.55 alone or p^b=0.49 in interaction with frequency). This indicates that outer hair cell functioning did not appear to change with aging.

There were also no obvious changes in the numbers of ribbon synapses between the inner hair cells (IHC) and auditory nerve fibers. We labeled presynaptic IHC ribbons and post-synaptic glutamate receptors (Figure 2B and Methods). Based on a custom-developed algorithm, the juxtaposition of pre- and post-synaptic structures was quantified from stacked confocal images. The number of synapses per IHC was plotted as a function of position from the cochlea apex in the 9- and 21-month-old animals (n=4 and n=5 respectively; Figure 2C). The number of synapses per IHC depended on the frequency (p^c=8e-4), increasing from fewer than 10 synapses to almost 20 synapses in the middle of the cochlea, and then decreasing again towards the base of the cochlea. The two curves that fitted the changes in the number of synapses as a function of position in the cochlea (p^d=0.93, interaction age and frequency p^e=0.72) are superimposed, indicating that numbers of synapses obtained for these two groups of animals were similar.

Auditory nerve and brainstem evaluations: CAP and ABRs

The mean CAP threshold of the auditory nerve did not change between the ages of nine and 21 months (Figure 3A, age effect p^f=0.54 alone or p^g=0.25 in interaction with frequency). At all suprathreshold levels (80 dB SPL, 60 dB SPL, 40 dB SPL), modest but nonsignificant decreases in CAP amplitude were observed for low frequencies after 15 months (interaction age and frequency, 80 dB: p^h=0.98; 60 dB p^{h2}=0.99; 40 dB p^{h3}=0.98, Figure 3B). Surprisingly, latency was slightly shorter at 21 months (age effect p^i=0.04 alone, 21 months vs. 15 months at 4 kHz p^j=3e-4, Figure 3C) and the effect was still visible at 60 dB SPL and 40 dB SPL, albeit not significant (age effect alone, 60 dB p^{i2}=0.46; 40 dB p^{i3}=0.06).

ABRs were quantified at visible wave II, typically associated with the cochlear nucleus responses (Chen and Chen, 1991). Contrasting with the relative stability of peripheral

thresholds, the ABR thresholds progressively changed (Figure 3D). At 15 months and at 21 months, there was a general increase in thresholds of maximum 15dB (age effect p^k<1e-10 alone and p^l=0.94 in interaction with frequency). For ABRs, we also observed a progressive, slight, decrease in amplitude for frequencies below 16 kHz (age effect alone 80 dB: p^m<1e-10; 60 dB: p^{m2}<1e-10; 40 dB: p^{m3}<1e-10; age effect in interaction with frequency 80 dB: p^n=0.13; 60 dB: p^{n2}=0.02; 40 dB: p^{n3}=5e-3). The ABR also confirmed the information provided by CAPs, indicating that latencies were unaffected (except at 60 dB where one p value is close to threshold) in the oldest animals (Figure 3F, Gi, Gii; age effect alone 80 dB: p^o=0.22; 60 dB: p^{o2}=0.04; 40 dB: p^{o3}=0.54, age effect in interaction with frequency p^p=0.31; 60 dB: p^{p2}=0.25; 40 dB: p^{p3}=0.78). Overall, we detected nonsignificant signs of aging for auditory nerve thresholds and amplitude values, and a more pronounced effect in the brainstem response (potentially corresponding to the cochlear nucleus).

Primary auditory cortex evaluation

Auditory thresholds

The mean cortical thresholds obtained for the three groups of animals are presented on Figure 4A. Cortical thresholds were slightly lower in the low- and high-frequencies than for ABRs, probably because different systems were used to collect these two sets of data (see Methods). In any case, there was no obvious difference in cortical thresholds between nine and 15 months of age (age effect p^q=0.8 alone and p^r=0.84 in interaction with frequency). By contrast, in 21-month-old animals, there was a pronounced general increase in thresholds (age effect p^s<1e-10 alone and p^t=0.38 in interaction with frequency). This increase was about 15-25 dB, except at 8 and 16 kHz.

Receptive field parameters

As shown in Figure 4B, from each spectro-temporal receptive fields (STRFs) collected at 75 dB SPL, several parameters were extracted, such as the value of the best frequency (BF), the 1st spike latency and duration of responses, tuning bandwidth and the ratio of maximal evoked firing rate to spontaneous activity (Figure 4B). Since the effects of aging on cortical thresholds and CAP/ABR parameters were not necessarily uniform across the hearing range, we split the analysis into three frequency bands, as a function of the BF of each recording: low frequency (LF, <8 kHz), mid-range frequency (MF, 8-20 kHz) and high frequency (HF, >20 kHz, see grey scale on bottom of Figure 4A). The number of cortical site recordings for each frequency band and each age group always exceeded 90 (Table 2).

We assessed the effect of aging on STRF parameters (Figures 4C-G). Multiple two-way ANOVAs were performed on age and BF group with interactions, for the five parameters shown in Figure 4C-G. We therefore applied Bonferroni correction to the significance threshold of the ANOVA tests, and the corrected threshold was 0.05/(5 x 3)=3.3e-3. The first spike latency was unaffected by aging (Figure 4C, $p^{u,v}\geq 0.01$ with or without interaction, note that latencies were again shorter, although not significantly so, for mid-range frequencies in the oldest animals, as for CAP and ABRs).. The response duration decreased for mid-range and high frequencies with aging, but this decrease was not statistically significant (Figure 4D, $p^{y,z}\geq 0.01$, with or without interaction. Tuning bandwidth at 75dB was narrower for oldest animals (Figures 4E; $p^{w}<1e\text{-}10$), with no significant interaction with frequency range (both $p^{x}=0.26$). Aging had no effect on the maximal evoked firing rate divided by baseline activity (Figure 4F, $p^{A,B}\geq 5.5e\text{-}3$ with or without interaction), and on the Q_{20dB} value, a measurement obtained from the frequency response area (FRA, Figure 4G, $p^{C,D}\geq 0.1$ with or without interaction).

These quantifications thus reveal modest and non-significant effects of aging on the maximum firing rate and duration, mostly at high frequencies. Aging significantly decreased tuning curve bandwidth at 75 dB SPL, probably due to the increase in cortical thresholds, but did not induce major changes in the overall shape of the tuning curves, as indicated by the lack of effect on the Q_{20dB} parameter.

Processing of communication sounds in the presence of noise

Communication sounds (such as the guinea-pig whistle and birdsong in our study) usually elicit neuronal discharges with very precise temporal spike patterns. Individual examples of evoked responses for these two types of vocalizations, in the presence and absence of three levels of background noise (at 60, 65 and 70 dB SPL) are displayed in Figure 5A. The example on the left illustrates tonic responses somewhat robust to noise, occurring in the presence of a high spontaneous discharge rate; the example on the right illustrates a phasic response that rapidly disappears in the presence of more noise. *CorrCoef* (an index of temporal precision, see Methods) was typically between 0.2 and 0.4 for both types of vocalization in the absence of noise. Age was associated with significantly lower *CorrCoef* values for both stimuli ($p^{E,F} \leq 7 \times 10^{-4}$) but this effect was observed only at 21 months, for both types of vocalization, and did not differ significantly across the frequency range of neurons (interaction age and frequency, $p^{G,H} > 0.28$).

At all ages, the *CorrCoef* values obtained for the two vocalizations were strongly decreased by additional noise, even at 60 dB SPL. LF neurons were more robust to additional noise than MF and HF neurons. However, the effect of aging disappeared when background noise was added (age effect alone or in interaction with frequency, $p^{I,J,K,L,M,N,O,P} > 0.04$, Bonferroni corrected threshold=0.05/(4 x 3)=4.2e-3).

To summarize, the temporal reliability of neuronal responses to natural stimuli were lower in 21-month-old animals in quiet conditions, but not in the presence of noise (potentially because the noise already produced a strong decrease in temporal reliability).

Gap detection

In both humans and animals, aging is known to alter the detection of small gaps inserted into acoustic signals (reviewed by (Walton, 2010). We investigated whether the auditory cortex neurons detected small gaps inserted into a natural stimulus (a guinea pig whistle) and whether aging impaired this detection. A whistle temporal envelope with the longest gap duration (64 ms, in green) is shown in Figure 6A. The post-stimulus time histograms (PSTHs)displayed below it correspond to a cortical recording, with responses to whistles containing gaps of 2 ms to 64 ms. A cortical site was considered to detect a gap if the firing rate in the 50 ms following the end of the gap increased to a level significantly above that immediately before the gap (red stars on Figure 6A), i.e., if the neuron had detected the second part of the stimulus after the gap. We determined the percentage of neurons detecting the different gap durations as a function of age (Figure 6B). For all gap durations, the neurons from all groups performed similarly (Figure 6B), and three-way ANOVA (age, gap duration, frequency band) confirmed that effect of age alone was not significant (p^Q=0.92). However, the interaction of aging with frequency was significant (p^R<1e-10). Indeed, we found that for gap durations≥16 ms, the oldest animals had a significantly higher gap detection percentage for LF neurons than the other groups (post-hoc 21 months vs. 9 months, p^S<2e-3, as well as gap duration 32ms, 21 months vs 15 months, p=6e-4). A smaller gap detection percentage was obtained for HF neurons, but this difference was not significant after Bonferroni correction (post-hoc 21 months vs. 9 or 15 months, 0.01<p^T<0.71, except gap duration 8ms,

21 months vs 15 months, p=4e-4). Surprisingly, the effect of aging detected here seems to be a small facilitation in gap detection for the LF neurons.

Temporal envelope processing

Figure 7A (left) displays neuronal responses to the presentation of amplitude-modulated white noise (100% modulation depth) at rates ranging from 2 to 50 Hz. This multi-unit recording generated clear onset responses up to 18 Hz, yielding vector strength (VS) values above 0.4 until this frequency. As classically observed in the auditory cortex (reviewed by (Joris et al., 2004), the vector strength value then decreased with increasing rate of amplitude modulation. The group results (Figure 7C) revealed that tMTFs were generally slightly better for the oldest animals (age effect alone p^U<1e-10), especially for high modulation frequencies.

We therefore averaged VS values over two ranges of temporal modulation frequencies [8-14] Hz and [20-32] Hz, splitting the results for each frequency band (LF, MF, HF, Figure 7D). The better tMTF values obtained for the [20-32] Hz modulation frequency range resulted from MF and HF neurons (age effect alone p^V<1e-10, post-hoc tests 21 months vs. 9 months, p^W<1e-4).

We then calculated VS values as a function of the depth of amplitude modulation (at 4 Hz) (Figure 7B). VS values typically decreased at lower depth modulation percentages (Figure 7E). As for tMTFs, we observed higher depth-MTFs for the oldest animals (Figure 7E), mostly for high modulation depths and MF neurons (Figure 7F). However, the overall age effect was not significant here (age alone p^X=0.05, in interaction with modulation frequency p^Y=0.33 or with frequency band of neurons p^Z=0.34). In any case, there was no steady, progressive degradation of dMTFs between the ages of nine and 21 months.

Principal component analysis for the cortical results

In the neurobiology of aging, a large interindividual variability is often reported for parameters quantified in aged subjects (e.g. see (Gleich et al., 2007; Getzmann et al., 2015) for hearing). We looked at 16 parameters derived from STRFs, responses to vocalizations, or amplitude-modulated sounds, and we analyzed the variability of these parameters in each age group. We first standardized each parameter, and we then plotted its variability for a given age (Figure 8A); the dashed lines on the plot indicate the confidence intervals. The oldest animals (21 months) did not display greater variability for any of the parameters tested. These findings were consistent with the mean inter-animal variability (averaged across all parameters), which was even smaller for the 21-month-old rats than for the other groups (Figure 8B, p^{α}=9e-4, post hoc 9 or 15 months vs. 21 months p^{β}<0.01).

Principal component analysis (PCA) can be used to describe the data when a large number of observations are coupled to a large number of variables, a situation in which it is not possible to present scatter plots for all the observations and variables. PCA creates new axes (called principal components, PCs) to represent the observations and the variables, accounting for as much of the variance as possible, with each PC orthogonal to the others. The contribution of each PC to the total variance can be used as a criterion to reduce the number of PCs involved in the new representation of the data (Figure 8C). PCA can also be used to visualize particular structures within observations or particular relationships between variables. We found that age had a significant effect mainly on components 2 and 4 (Figure 8D). Those two components are represented in Figure 8E. The age effect is illustrated by the distance between the clusters of points (in colors). This analysis shows that some groups of variables displayed similar patterns of change in relation with aging (and therefore parallel to the direction of the age effect). This was the case for tMTF and Depth-MTF quantified with vector strength, for which aging led to somewhat better results. In the opposite direction, one

can find CorrCoef (the index used to quantify the temporal reliability at presentation of vocalizations presented in silence or in the presence of white noise) bandwidth and duration of STRFs, all of them rather showing lower performance of neurons for the oldest animals. In addition, results extracted from STRFs, gap detection and responses to vocalizations were orthogonal (i.e. not correlated) to those related to temporal processing (tMTFs, depth-MTFs). Those results are therefore consistent with the previous studies and did not reveal hidden correlations between studies variables. However, one striking feature that emerged from the PCA analysis was the considerable overlap between the clusters of points corresponding to the different age groups. Age did not have a significant effect on the first component (p^{δ}=0.92), which accounted for 22% of the variability and mainly had a significant effect on the second and fourth components (p^{γ}<1.1e-6), which accounted only for 24% of the variability. Even on the components 2 and 4, the group centers could be found within 1 SD of other groups as shown in Figure 8E. PCA showed that the variability of measurements within groups was very high with respect to that between groups. Consistent with many of the studies cited above, aging had an effect on the parameters extracted from the responses of auditory cortex neurons, but it was not massive and was limited to the 21-month-old rat group.

GABAergic inhibitory neurotransmission

During aging, neurochemical changes take place in the central auditory system, including a downregulation of glycinergic and GABAergic inhibitory neurotransmission from the brainstem to the cortex (Caspary et al., 2008). These changes can affect the functional properties of cortical cells in either the spectral (Wang et al., 2000) or temporal domain (Kurt et al., 2006). We quantified GAD67 labeling (one of the two enzymes responsible for GABA synthesis) in the primary auditory cortex of animals at 9, 15 and 21 months of age (n = 4-6 in the different groups) (Figure 9). We analyzed the numbers of labeled cells in the

supragranular (II-III, labeled Sup) and infragranular layers (V-VI, labeled Deep). We observed a small, but non-significant, decrease in GAD labeling with aging (p^{ε}=0.09; Figure 7B). There was no significant effect of the factor "layer" (p^{ζ}=0.59) and no interaction between age and layer (p^{η}=0.47), suggesting that the small, but non-significant decrease in the number of GABAergic neurons occurred in all layers of the cortex. GAD 67 labeling was highly variable in the 21-month-old animals and variability differed significantly between ages (p^{θ}=0.02).

Performance in a task involving discrimination between different modulation depths

As we recorded neural responses to amplitude-modulated noise with various levels of modulation depth (see Figure 7), we also tested the ability of animals to distinguish between such stimuli in a behavioral task (Figure 10A). We assessed the ability of animals aged 9, 15 and 21 months to discriminate between constant white noise and different levels of amplitude-modulated white noise (Figure 10A, same levels of modulation as in Figure 7). The last point on the left of Figure 10B indicates the percentage of animals failing to achieve three successive sessions with values of A' > 0.75, even in the easiest conditions (a constant white noise vs. a 100% depth modulated-white noise). The other points indicate the percentage of animals reaching this criterion for depths of amplitude modulation ranging from 100% (second point from left) to 20% (last point on the right). Our animals did not perform as well as in another study testing the same amplitude modulation thresholds (Kelly et al., 2006) which used an appetitive conditioning as well as a longer training duration, but this did not prevent us to observe effects of aging. Indeed, failure (i.e. the percentage of animals unable to learn the task) increased with aging. A few nine- and 15-month-old animals were able to achieve the most difficult level of differentiation, discriminating between a 20% depth

amplitude-modulated white noise and constant white noise. By contrast, none of the 21-month-old animals was able to do this, and only one of the animals of this group was able to achieve a satisfactory performance with a 60% depth of amplitude modulation. We checked for significant differences between the distributions corresponding to the different groups and compensated for the small numbers of animals in each category by grouping together, for each age, the performances obtained for 100% and 80% modulation depths and those obtained for 60, 40 and 20% modulation depths. The distributions did not differ significantly between the nine- and 15-month-old animals (p^{ι} =0.35) but performance distributions differed significantly between the nine- and 21-month-old animals (p^{κ}=0.01), suggesting that the oldest animals had the poorest discrimination performances.

The lower performance of the oldest animals may have resulted from a perceptual deficit, a cognitive deficit, or motor alterations, because our task required that the animals to move into the other compartment of the shuttle box within five seconds. We investigated possible impairment of motor responses even when correctly responding, by analyzing the 10 shortest latencies per animal in response to the CS+ (the amplitude modulated white noise) signal when the animals had learnt to discriminate between constant white noise and 100% depth of amplitude modulation (after 3 successful sessions). Response latency differed between age groups (p^{λ}=9e-4): response latencies were similar (about 2 s) in the nine- and 15-month-old animals (p^{μ}=0.52), but the 21-month-old animals took significantly longer to move to the safe compartment ($p^{\nu,\xi}\leq$9e-3) (Figure 10C). These findings suggest that the aged animals may have also displayed a motor, cognitive, or behavioral impairment.

Discussion

Based on ABRs and cortical recordings, we detected modest, late, effects of aging on auditory thresholds, whereas peripheral measurements (CAP, DPOAE and the number of ribbon synapses) revealed no effect of aging. ABR and cortical thresholds were partially preserved at 8 and 16 kHz, whereas thresholds increased by up to 30 dB at lower and higher frequencies. These threshold shifts were accompanied by modest alterations to receptive field parameters (bandwidth). At 21 months of age (estimated to represent 80-90% of the lifespan for Sprague-Dawley rats), changes in cortical responses to heterospecific communication sounds were observed. When these vocalizations were presented in the presence of background noise, there was no global effect of aging. Surprisingly, aging appeared to have no deleterious effect on temporal processing (gap detection, temporal and depth modulation transfer functions). A PCA performed on a large number of parameters indicated that the inter-animal variability was large relative to the variability across groups of ages. An immunohistochemical study revealed a non-significant decrease in $GAD67^{+}$ labeling in all cortical layers. Finally, the performance of aged rats was lower than younger rats in a behavioral task (detection of modulation depths in the signal envelope). Most of our results, from peripheral measurements to behavioral evaluations, showed no difference between nine- and 15-month-old rats, suggesting that aging has no effect before the age of 15 months at the earliest in this rat strain.

Methodological issues

Many previous studies have used multi-unit recordings to characterize the functional properties of auditory cortex neurons (e.g., (Brosch and Schreiner, 1997; Escabí and Read, 2003; Noreña and Eggermont, 2005; Tillein et al., 2016), including the temporal properties of cortical neurons (Cotillon and Edeline, 2000; Cotillon et al., 2000; Cotillon-Williams and

Edeline, 2003; Imaizumi et al., 2010; Johnson et al., 2012). It could be argued that this type of recording prevented us from detecting small age-related alterations. However, we were able, with this type of recording, to dissociate the cortical effects of different noradrenergic agonists (Gaucher and Edeline, 2015) and to detect discrimination between vowels of very brief durations (Occelli et al., 2016), suggesting that subtle differences are detectable even with MUA recordings.

We used Sprague Dawley rats rather than the rat model classically used for aging studies, the Fisher 344 rat, because the Sprague Dawley rat strain is the most widely used for behavioral studies. Furthermore, we used only female rats, raising questions about the likelihood of obtaining similar results for male animals (e.g. see (Costa et al., 2016). This is clearly an important issue, but it should not attenuate the main message of this study: in the absence of peripheral alterations, only modest effects were observed in the brainstem and cortex.

Electrophysiological correlates of aging in the auditory system

Only modest effects of aging on the auditory system were detected here: hearing loss ranged from 20 dB in the cortex, to 15 dB in the brainstem level and zero in the periphery (based on CAP and DPOAEs). We also detected no decrease in the number of synapses per inner hair cell, suggesting that these animals had unimpaired afferent innervation, contrary to old mice (Stamataki et al., 2006). Here, the brainstem and cortical thresholds remained stable until the age of 15 months, and marked hearing loss was observed only at 21 months.

In contrast, major age-related modifications have been described in the lower levels of the auditory system (review in (Boettcher, 2002). Increases in ABR thresholds and response latencies, and decreases in response magnitude are the most classically reported effects of aging (Dum, 1983; Boettcher et al., 1993a, 1993b; Walton et al., 1995; Turner and Willott,

1998; Gourévitch and Edeline, 2011; Ng et al., 2015). Threshold increases have also been detected in the cortex (Gourévitch and Edeline, 2011). Temporal processing also seems to be altered in the brainstem, as shown by a deficit in gap detection according to ABRs (Williamson et al., 2015) and by changes in the response to amplitude-modulated sounds in the inferior colliculus (Palombi and Caspary, 1996a, 1996b; Walton et al., 2002). Alterations in evoked responses have suggested a possible decrease in inhibition during aging (review in (Caspary et al., 2008): in the colliculus, the age-related decrease in response latency to AM stimuli (Simon et al., 2004) and the attenuation of direction selectivity (Costa et al., 2016) may also stem from reduced inhibition. Similarly, the increase in response duration observed in the auditory cortex of aged guinea pigs may result from a decrease in intracortical feedforward inhibition (Gourévitch and Edeline, 2011). This hypothesis is supported by the findings of several studies reporting an increase in spontaneous activity with aging, from the cochlear nucleus (Frisina and Walton, 2006) and inferior colliculus (Willott et al., 1988) to the auditory cortex (Hughes et al., 2010). The alteration of receptive field structure (Turner et al., 2005) and the apparent lack of response suppression around the CF (Caspary et al., 2005) may also be accounted for by a decrease in inhibition.

Other studies have reported only modest effects of aging on physiological responses. Willot and colleagues observed considerable variability in the age-related hearing loss measured by ABR evaluations, depending on the mouse strain (Turner and Willott, 1998; Willott and Turner, 1999; Willott et al., 2000). In some mouse strains (C57Bl/6), animals can be partially deaf by the time they are a few weeks old, whereas in other strains (CBA/j), hearing seems to remain unimpaired for many months. Furthermore, only modest hearing loss has been detected by ABR measurements in geriatric macaque monkeys (Ng et al., 2015). Subtle effects on direction selectivity were observed in the cortex of aged monkeys (Juarez-Salinas et

al., 2010). In addition, Fischer brown Norway rats display no effect of aging on thalamic responses in a stimulus-specific adaptation protocol (Richardson et al., 2013).

The receptive field alterations described here (decrease in bandwidth) may be explained by the increase in auditory cortical thresholds. By contrast, the stability or improvement in temporal processing observed here in the gap detection protocol and for tMTF and Depth-MTF determinations seems to contradict the results of previous studies (Mendelson and Ricketts, 2001; Lee et al., 2002; Mendelson and Lui, 2004). However, these and other studies (Turner et al., 2005; Hughes et al., 2010) described cortical alterations without documenting peripheral hearing loss in the animals concerned (or at least the effects on the brainstem). In fact, old male Sprague Dawley rats displaying peripheral alterations (a decrease in DPOAE amplitude) also displayed broader orientation and spectral selectivity in the superior colliculus (Costa et al., 2016, 2017). In these studies, 22-month-old rats displayed a larger increase in ABR threshold (15-30 dB) than in our study, possibly due to differences between the sexes or housing conditions (our animals were aged in our own animal facilities with a known low level of background noise). Thus, the lack of prominent cortical effects in our study may be a direct consequence of the stability of our peripheral thresholds. In our study, CAP and DPOAE measurements were quite stable, and the late emergence of alterations to the brainstem and cortex should therefore be seen as a signature of the central effects of aging, and not as a combination of central aging and hearing loss. Modest changes in cortical physiology in oldest animals could be attributed to the non-significantly diminished CAP or significantly diminished ABR wave II amplitudes documented in Figure 3B and 3E. Fifteen-month-old rats also displayed diminished ABR wave II amplitudes but their cortical activity was not altered. This discrepancy could be explained by a similar mechanism to that found in Möhrle et al., (2016) where it was suggested that young to middle-aged animals (unlike old ones) could centrally compensate for a decrease of auditory fiber activity related

to inner hair cell synaptopathy. In any case, latencies or firing rates measured in the primary auditory cortex were shown to be orthogonal to aging effects (Figure 8E) according to the PCA performed on our cortical data. This PCA revealed a significant difference between old and young animals (only for the 2^{nd} and 4^{th} components), but inter-animal and inter-neuron variability remained very high relative to the difference between groups. Surprisingly, this analysis also indicated that inter-individual variability decreased with aging, whereas studies in humans have reported an increase in inter-individual variability with aging (review in (Füllgrabe et al., 2014), see also (Paraouty and Lorenzi, 2017). However, human subjects have heterogeneous genetic backgrounds, whereas we worked on rats with a homogeneous genetic background, potentially accounting for the differences between our results and those for humans.

Relationship with psychoacoustic data

Our analyses of tMTF and depth-MTF revealed an absence of deleterious effects of aging on temporal processing. This is in line with Paraouty and Lorenzi (2017) who found no effect of aging on the detection of amplitude-modulated sound in a large cohort of subjects. However, we should bear in mind that in the results of psychoacoustic studies depend not only on auditory system performance, but also on processing steps, such as attention and decision-making, which are also affected by aging (Füllgrabe et al., 2014; Huang et al., 2015; Strough et al., 2015). The deficits in psychoacoustic tasks observed in humans may be due to a decline of attentional and cognitive abilities (review in Fullgrabe et al. 2014). Similarly, the decrease in behavioral performance observed here in the 21-month-old animals may result from a decline of attentional and cognitive abilities, rather than from a loss of hearing. Indeed, response latencies in the task increased with aging (Figure 10C), whereas cortical recordings

showed no decrease in depth-modulated noise processing (Figure 7D-F), suggesting an impairment of motor or cognitive abilities.

In the past, psychophysical results have suggested that aging is associated with hearing impairment and with deficits in the processing of the temporal parameters of sound. In addition, elderly subjects often experience major difficulties understanding speech in adverse listening situations, sometimes even in the absence of high audiometric thresholds (for review, see (Füllgrabe et al., 2014; Schoof and Rosen, 2014). This situation may result from changes in suprathreshold auditory processing (for review, see (Fitzgibbons and Gordon-Salant, 2010), which could be explained by high-threshold auditory nerve fibers being the first to be affected during aging (Sergeyenko et al., 2013). However, several studies have indicated that frequency selectivity does not change with age provided that audiometric thresholds remain normal (Lutman et al., 1991; Moore et al., 1992; Hopkins and Moore, 2011), suggesting that modulated signal processing should be similar in younger and older listeners with similar thresholds.

Immunohistochemical markers of age-related changes and conclusion

Here, we detected a small decrease in GAD67 labeling with aging, consistent with the findings of previous studies (Ling et al., 2005; Burianova et al., 2009). However, this decrease was not statistically significant. It also remains unclear whether such changes are specific to the GABAergic system. Several GABAergic subpopulations have been characterized in the auditory cortex. In aged rats, cortical neurons expressing $GABA_A$ receptors tend to have lower levels of α1, β1, β2, γ1, γ2s, and γ2L subunit protein and mRNA (Caspary et al., 2013). Age-related changes in parvalbumin-positive neuron levels may be species-dependent or even strain-dependent: their number seems to increase with age in Long Evans rats, whereas they

seem to decrease with age in the auditory cortex of Fischer F344 rats (Ouda et al., 2008) and in the brainstem of non-human primates (Engle et al., 2014; Gray et al., 2014). The neuronal expression of GAD65 and GAD67 has been reported to decrease during aging (Ling et al., 2005; Burianova et al., 2009). In addition, the numbers of neurons positive for somatostatin, calbindin and calretinin decrease with aging throughout the central auditory system in rats and primates (Gray et al., 2014; Ouda et al., 2012, 2008; Ouellet and de Villers-Sidani, 2014). One recent study showed that age-related synaptic response alterations in the auditory thalamus involved both a decrease in the total number of nicotinic receptors (nACh), and a switch from high- to low-affinity nACh receptors (Sottile et al., 2017). Thus, future studies may reveal that aging affects not only inhibitory neurotransmission, but also many other neurotransmitters.

To conclude, and based on functional and anatomical data, we show here that the peripheral auditory system of female Sprague Dawley rats changes little, if at all, with aging. These findings are consistent with observations indicating that the effect of aging is strain-dependent and that not all aging scenarios lead to major changes. As a simplification, the peripheral system acts essentially as a signal detector, whereas the central system processes complex acoustic features. Animal models in which aging does not affect the signal detector provide us with a unique opportunity to dissect the consequences of "central aging" in isolation (i.e., the effects of aging on the extraction of acoustic features by central networks). Here, we show that, when peripheral processing is little affected, intrinsic central aging of the auditory system exists but is modest, at least in female Sprague-Dawley rats. Obviously, aging in the central nervous system involves a myriad of mechanisms ranging from the molecular (Lenaz et al., 2002; Mattson and Liu, 2002; Penney and Tsai, 2014; Deibel et al., 2015) to the synaptic (Villanueva-Castillo et al., 2017) level. Potential changes in the

functions of the microglia (reviewed in (Colonna and Butovsky, 2017) and extracellular matrix (Sethi and Zaia, 2017; Song and Dityatev, 2017) should also be taken into account. If we wish to understand the effects of aging on auditory function, we will need to study different levels of auditory information processing in the same animals, with different techniques. This study can serve as a starting point.

Appendix

Details of each statistical test

Index of pvalues	Type of test	df1,df2	Statistics	pvalue
a	ANOVA two-way age x frequency with interaction, age effect	1,882	F=0.36	0.55
b	ANOVA two-way age x frequency with interaction, age x frequency effect	20,882	F=0.98	0.49
c	ANOVA two-way age x frequency with interaction, frequency effect	1,49	F=12.67	8.10^{-4}
d	ANOVA two-way age x frequency with interaction, age effect	1,49	F=0.01	0.93
e	ANOVA two-way age x frequency with interaction, age x frequency effect	1,49	F=0.13	0.72
f	ANOVA two-way age x frequency with interaction, age effect	1,113	F=0.38	0.54
g	ANOVA two-way age x frequency with interaction, age x frequency effect	6,113	F=1.33	0.25
h	ANOVA two-way age x frequency with interaction, age x frequency effect	6,109	F=0.16	0.98
h2	ANOVA two-way age x frequency with interaction, age x frequency effect	6,109	F=0.08	0.99
h3	ANOVA two-way age x frequency with interaction, age x frequency effect	6,109	F=0.18	0.98
i	ANOVA two-way age x frequency with interaction, age effect	1,113	F=4.21	0.04
i2	ANOVA two-way age x frequency with interaction, age effect	1,113	F=0.56	0.46
i3	ANOVA two-way age x frequency with interaction, age effect	1,113	F=3.71	0.06
j	Unpaired *t*-test, Tukey-Kramer correction, 15 m vs. 21 m	11	T=-5.15	3.10^{-4}
k	ANOVA two-way age x frequency with interaction, age effect	1,133	F=27.05	<1e-10
l	ANOVA two-way age x frequency with interaction, age x frequency effect	6,133	F=0.3	0.94
m	ANOVA two-ways age * frequency with interaction, age effect	1,133	F=79.74	<1e-10
n	ANOVA two-way age x frequency with interaction, age x frequency effect	6,133	F=1.7	0.13
m2	ANOVA two-ways age * frequency with interaction, age effect	1,133	F=74.88	<1e-10
n2	ANOVA two-way age x frequency with interaction, age x frequency effect	6,133	F=2.7	0.02
m3	ANOVA two-ways age * frequency with interaction, age effect	1,133	F=55.1	<1e-10
n3	ANOVA two-way age x frequency with interaction, age x frequency effect	6,133	F=3.2	5e-3
o	ANOVA two-way age x frequency with interaction, age effect	1,133	F=1.51	0.22
p	ANOVA two-way age x frequency with interaction, age x frequency effect	6,133	F=1.2	0.31
o2	ANOVA two-way age x frequency with interaction, age effect	1,126	F=4.43	0.04
p2	ANOVA two-way age x frequency with interaction, age x frequency effect	6,126	F=1.32	0.25
o3	ANOVA two-way age x frequency with interaction, age effect	1,129	F=0.37	0.54
p3	ANOVA two-way age x frequency with interaction, age x frequency effect	6,129	F=0.53	0.78
q	ANOVA two-way age x frequency with interaction, age effect (only 9 and 15 months)	1,361	F=0.06	0.8
r	ANOVA two-way age x frequency with interaction, age x frequency effect (only 9 and 15 months)	24,361	F=0.72	0.84

s	ANOVA two-way age x frequency with interaction, age effect	1,552	F=105.8	<1e-10
t	ANOVA two-way age x frequency with interaction, age x frequency effect	24,552	F=1.06	0.38
u	ANOVA two-way age x BF group with interaction, age effect	1,1165	F=0.13	0.72
v	ANOVA two-way age x BF group with interaction, age x BF group effect	2,1165	F=4.28	0.01
w	ANOVA two-way age x BF group with interaction, age effect	1,1165	F=82.12	<1e-10
x	ANOVA two-way age x BF group with interaction, age x BF group effect	2,1165	F=1.34	0.26
y	ANOVA two-way age x BF group with interaction, age effect	1,1165	F=6.08	0.01
z	ANOVA two-way age x BF group with interaction, age x BF group effect	2,1165	F=2.58	0.08
A	ANOVA two-way age x BF group with interaction, age effect	1,1165	F=0.56	0.45
B	ANOVA two-way age x BF group with interaction, age x BF group effect	2,1165	F=5.23	$5.5e^{-3}$
C	ANOVA two-way age x BF group with interaction, age effect	1,1120	F=2.7	0.1
D	ANOVA two-way age x BF group with interaction, age x BF group effect	2,1120	F=0.01	0.99
E	ANOVA two-way age x BF group with interaction, age effect	1,772	F=11.49	7e-4
F	ANOVA two-way age x BF group with interaction, age effect	1,569	F=17.57	<1e-10
G	ANOVA two-way age x BF group with interaction, age effect	2,772	F=0.24	0.79
H	ANOVA two-way age x BF group with interaction, age effect	2,569	F=1.27	0.28
I	ANOVA two-way age x BF group with interaction, age effect (Whistle, 60 dB Noise)	1,760	F=1.97	0.16
J	ANOVA two-way age x BF group with interaction, age x BF group effect (Whistle, 60 dB Noise)	2,760	F=0.83	0.43
K	ANOVA two-way age x BF group with interaction, age effect (Whistle, 70 dB Noise)	1,755	F=0.08	0.78
L	ANOVA two-way age x BF group with interaction, age x BF group effect (Whistle, 70 dB Noise)	2,755	F=0.17	0.84
M	ANOVA two-way age x BF group with interaction, age effect (Birdsong, 60 dB Noise)	1,561	F=3.9	0.05
N	ANOVA two-way age x BF group with interaction, age x BF group effect (Birdsong, 60 dB Noise)	2,561	F=0.98	0.38
O	ANOVA two-way age x BF group with interaction, age effect (Birdsong, 70 dB Noise)	1,554	F=4.19	0.04
P	ANOVA two-way age * BF group with interaction, age x BF group effect (Birdsong, 70 dB Noise)	2,554	F=0.92	0.4
Q	ANOVA three-way age x gap duration x BF group with pair interactions, age effect	1,7178	F=0.1	0.92
R	ANOVA three-way age x gap duration x BF group with pair interactions, age x BF group effect	2,7178	F=22.82	<1e-10
S	Unpaired *t*-test, Bonferroni correction, 9 m vs. 21 m, gap durations≥16 ms	>189	T>3.11	<2e-3
T	Unpaired *t*-test, Bonferroni correction, 9 m vs. 21 m or 15 m vs. 21 m, all gap durations (except gap duration 8ms, 21 m vs 15 m)	>246	-2.45>T>-0.38	0.01<p<0.71
U	ANOVA three-way age x TMF x BF group with pair interactions, age effect	1,13014	F=30.93	<1e-10
V	ANOVA two-way age x BF group with interaction, age effect	1,808	F=23.18	<1e-10
W	Unpaired *t*-test, Bonferroni correction, 9 m vs. 21 m, modulation frequency range [20-32] Hz	>205	T>4.08	<1e-4
X	ANOVA three-way age x DMF x BF group with pair interactions, age effect	1,7574	F=4.01	0.05
Y	ANOVA three-way age x DMF x BF group with pair interactions, age x DMF effect	1,7574	F=0.95	0.33
Z	ANOVA three-way age x DMF x BF group with pair interactions, age x BF effect	2,7574	F=1.09	0.34
α	ANOVA one-way age effect	2,45	F=8.17	9e-4
β	Unpaired *t*-test, 9 or 15 m vs. 21 m	30	T>2.61	<0.01

γ	ANOVA one-way age effect	2,585	F>14	<1.1e-6
δ	ANOVA one-way age effect	2,585	F=0.08	0.92
ε	ANOVA two-way age x layer depth with interactions, age effect	1,28	F=3.12	0.09
ζ	ANOVA two-way age x layer depth with interactions, layer effect	1,28	F=0.35	0.56
η	ANOVA two-way age x layer depth with interactions, age effect	1,28	F=0.53	0.47
θ	LEVENE test, depth layers pooled, age effect	2,29	F=4.23	0.02
ι	Chi^2	2	C=2.09	0.35
κ	Chi^2 test	2	C=8.58	0.01
λ	ANOVA one way, age effect	3,107	F=5.92	8.10^{-4}
μ	Unpaired *t*-test, Tukey-Kramer correction, 9 m vs. 15 m	3,107	T=0.21	0.52
ν	Unpaired *t*-test, Tukey-Kramer correction, 9 m vs. 21 m	3,107	T=-0.59	9e-3
ξ	Unpaired *t*-test, Tukey-Kramer correction, 15 m vs. 21 m	3,107	T=-0.8	1e-3

References

Batrel C, Huet A, Hasselmann F, Wang J, Desmadryl G, Nouvian R, Puel J-L, Bourien J (2017) Mass Potentials Recorded at the Round Window Enable the Detection of Low Spontaneous Rate Fibers in Gerbil Auditory Nerve. PLOS ONE 12:e0169890.

Blanca MJ, Alarcón R, Arnau J (2017) Non-normal data: Is ANOVA still a valid option? Psicothema:552–557.

Boettcher FA (2002) Presbyacusis and the auditory brainstem response. J Speech Lang Hear Res 45:1249–1261.

Boettcher FA, Mills JH, Norton BL (1993a) Age-related changes in auditory evoked potentials of gerbils. I. Response amplitudes. Hear Res 71:137–145.

Boettcher FA, Mills JH, Norton BL, Schmiedt RA (1993b) Age-related changes in auditory evoked potentials of gerbils. II. Response latencies. Hear Res 71:146–156.

Bourien J, Tang Y, Batrel C, Huet A, Lenoir M, Ladrech S, Desmadryl G, Nouvian R, Puel J-L, Wang J (2014) Contribution of auditory nerve fibers to compound action potential of the auditory nerve. J Neurophysiol 112:1025–1039.

Brosch M, Schreiner CE (1997) Time course of forward masking tuning curves in cat primary auditory cortex. J Neurophysiol 77:923–943.

Brudzynski SM (2009) Communication of adult rats by ultrasonic vocalization: biological, sociobiological, and neuroscience approaches. ILAR J 50:43–50.

Burianova J, Ouda L, Profant O, Syka J (2009) Age-related changes in GAD levels in the central auditory system of the rat. Exp Gerontol 44:161–169.

Caspary DM, Hughes LF, Ling LL (2013) Age-related GABAA receptor subunit changes in rat auditory cortex. Neurobiol Aging 34:1486–1496.

Caspary DM, Ling L, Turner JG, Hughes LF (2008) Inhibitory neurotransmission, plasticity and aging in the mammalian central auditory system. J Exp Biol 211:1781–1791.

Caspary DM, Schatteman TA, Hughes LF (2005) Age-related changes in the inhibitory response properties of dorsal cochlear nucleus output neurons: role of inhibitory inputs. J Neurosci Off J Soc Neurosci 25:10952–10959.

Chen T-J, Chen S-S (1991) Generator study of brainstem auditory evoked potentials by a radiofrequency lesion method in rats. Exp Brain Res 85:537–542.

Ciorba A, Bianchini C, Pelucchi S, Pastore A (2012) The impact of hearing loss on the quality of life of elderly adults. Clin Interv Aging Available at: https://www.dovepress.com/the-impact-of-hearing-loss-on-the-quality-of-life-of-elderly-adults-peer-reviewed-article-CIA [Accessed May 4, 2017].

Clinard CG, Tremblay KL, Krishnan AR (2010) Aging alters the perception and physiological representation of frequency: Evidence from human frequency-following response recordings. Hear Res 264:48–55.

Colonna M, Butovsky O (2017) Microglia Function in the Central Nervous System During Health and Neurodegeneration. Annu Rev Immunol 35:441–468.

Costa M, Lepore F, Guillemot J-P (2017) Spectral and temporal auditory processing in the superior colliculus of aged rats. Neurobiol Aging 57:64–74.

Costa M, Lepore F, Prévost F, Guillemot J-P (2016) Effects of aging on peripheral and central auditory processing in rats. Eur J Neurosci 44:2084–2094.

Cotillon N, Edeline JM (2000) Tone-evoked oscillations in the rat auditory cortex result from interactions between the thalamus and reticular nucleus. Eur J Neurosci 12:3637–3650.

Cotillon N, Nafati M, Edeline JM (2000) Characteristics of reliable tone-evoked oscillations in the rat thalamo-cortical auditory system. Hear Res 142:113–130.

Cotillon-Williams N, Edeline J-M (2003) Evoked Oscillations in the Thalamo-Cortical Auditory System Are Present in Anesthetized but not in Unanesthetized Rats. J Neurophysiol 89:1968–1984.

Davis RK, Stevenson GT, Busch KA (1956) Tumor Incidence in Normal Sprague-Dawley Female Rats. Cancer Res 16:194–197.

Deibel SH, Zelinski EL, Keeley RJ, Kovalchuk O, McDonald RJ, Deibel SH, Zelinski EL, Keeley RJ, Kovalchuk O, McDonald RJ (2015) Epigenetic alterations in the suprachiasmatic nucleus and hippocampus contribute to age-related cognitive decline. Oncotarget 6:23181–23203.

Dum N (1983) Effects of age upon auditory evoked potentials from the inferior colliculus and cortex in the guinea pig. Arch Otorhinolaryngol 238:251–261.

Durbin PW, Williams MH, Jeung N, Arnold JS, Parrott MW, Davis T (1966) Development of Spontaneous Mammary Tumors over the Life-Span of the Female Charles River (Sprague-Dawley) Rat: The Influence of Ovariectomy, Thyroidectomy, and Adrenalectomy-Ovariectomy. Cancer Res 26:400–411.

Engineer CT, Perez CA, Chen YH, Carraway RS, Reed AC, Shetake JA, Jakkamsetti V, Chang KQ, Kilgard MP (2008) Cortical activity patterns predict speech discrimination ability. Nat Neurosci 11:603–608.

Engle JR, Gray DT, Turner H, Udell JB, Recanzone GH (2014) Age-related neurochemical changes in the rhesus macaque inferior colliculus. Front Aging Neurosci 6 Available at: http://journal.frontiersin.org.gate2.inist.fr/article/10.3389/fnagi.2014.00073/full [Accessed May 16, 2017].

Engle JR, Recanzone GH (2012) Characterizing spatial tuning functions of neurons in the auditory cortex of young and aged monkeys: a new perspective on old data. Front Aging Neurosci 4:36.

Escabí MA, Read HL (2003) Representation of spectrotemporal sound information in the ascending auditory pathway. Biol Cybern 89:350–362.

Fay MP, Freedman LS, Clifford CK, Midthune DN (1997) Effect of Different Types and Amounts of Fat on the Development of Mammary Tumors in Rodents: A Review. Cancer Res 57:3979–3988.

Fitzgibbons PJ, Gordon-Salant S (2010) Age-related differences in discrimination of temporal intervals in accented tone sequences. Hear Res 264:41–47.

Freedman LS, Clifford C, Messina M (1990) Analysis of Dietary Fat, Calories, Body Weight, and the Development of Mammary Tumors in Rats and Mice: A Review. Cancer Res 50:5710–5719.

Frisina DR, Frisina RD (1997) Speech recognition in noise and presbycusis: relations to possible neural mechanisms. Hear Res 106:95–104.

Frisina RD, Walton JP (2006) Age-related structural and functional changes in the cochlear nucleus. Hear Res 216–217:216–223.

Füllgrabe C, Moore BCJ, Stone MA (2014) Age-group differences in speech identification despite matched audiometrically normal hearing: contributions from auditory temporal processing and cognition. Front Aging Neurosci 6 Available at: https://www-ncbi-nlm-nih-gov.gate2.inist.fr/pmc/articles/PMC4292733/ [Accessed May 17, 2017].

Gates GA, Mills JH (2005) Presbycusis. Lancet 366:1111–1120.

Gaucher Q, Edeline J-M (2015) Stimulus-specific effects of noradrenaline in auditory cortex: implications for the discrimination of communication sounds. J Physiol 593:1003–1020.

Gaucher Q, Huetz C, Gourévitch B, Edeline J-M (2013) Cortical inhibition reduces information redundancy at presentation of communication sounds in the primary auditory cortex. J Neurosci Off J Soc Neurosci 33:10713–10728.

Getzmann S, Wascher E, Falkenstein M (2015) What does successful speech-in-noise perception in aging depend on? Electrophysiological correlates of high and low performance in older adults. Neuropsychologia 70:43–57.

Gleich O, Kittel MC, Klump GM, Strutz J (2007) Temporal integration in the gerbil: The effects of age, hearing loss and temporally unmodulated and modulated speech-like masker noises. Hear Res 224:101–114.

Goldberg JM, Brown PB (1969) Response of binaural neurons of dog superior olivary complex to dichotic tonal stimuli: some physiological mechanisms of sound localization. J Neurophysiol 32:613–636.

Gourévitch B, Edeline J-M (2011) Age-related changes in the guinea pig auditory cortex: relationship with brainstem changes and comparison with tone-induced hearing loss. Eur J Neurosci 34:1953–1965.

Gratton MA, Bateman K, Cannuscio JF, Saunders JC (2008) Outer- and middle-ear contributions to presbycusis in the Brown Norway rat. Audiol Neurootol 13:37–52.

Gray DT, Engle JR, Recanzone GH (2014) Age-Related Neurochemical Changes in the Rhesus Macaque Cochlear Nucleus. J Comp Neurol 522:1527–1541.

Harris KC, Eckert MA, Ahlstrom JB, Dubno JR (2010) Age-related differences in gap detection: effects of task difficulty and cognitive ability. Hear Res 264:21–29.

Hellstrom LI, Schmiedt RA (1996) Measures of tuning and suppression in single-fiber and whole-nerve responses in young and quiet-aged gerbils. J Acoust Soc Am 100:3275–3285.

Helzner EP, Cauley JA, Pratt SR, Wisniewski SR, Zmuda JM, Talbott EO, de Rekeneire N, Harris TB, Rubin SM, Simonsick EM, Tylavsky FA, Newman AB (2005) Race and Sex Differences in Age-Related Hearing Loss: The Health, Aging and Body Composition Study. J Am Geriatr Soc 53:2119–2127.

Hopkins K, Moore BCJ (2011) The effects of age and cochlear hearing loss on temporal fine structure sensitivity, frequency selectivity, and speech reception in noise. J Acoust Soc Am 130:334–349.

Huang YH, Wood S, Berger DE, Hanoch Y (2015) Age differences in experiential and deliberative processes in unambiguous and ambiguous decision making. Psychol Aging 30:675–687.

Huetz C, Philibert B, Edeline JM (2009) A spike-timing code for discriminating conspecific vocalizations in the thalamocortical system of anesthetized and awake guinea pigs. J Neurosci 29:334–350.

Hughes LF, Turner JG, Parrish JL, Caspary DM (2010) Processing of broadband stimuli across A1 layers in young and aged rats. Hear Res.

Humes LE, Dubno JR, Gordon-Salant S, Lister JJ, Cacace AT, Cruickshanks KJ, Gates GA, Wilson RH, Wingfield A (2012) Central presbycusis: a review and evaluation of the evidence. J Am Acad Audiol 23:635–666.

Imaizumi K, Priebe NJ, Sharpee TO, Cheung SW, Schreiner CE (2010) Encoding of Temporal Information by Timing, Rate, and Place in Cat Auditory Cortex. PLOS ONE 5:e11531.

Johnson JS, Yin P, O'Connor KN, Sutter ML (2012) Ability of primary auditory cortical neurons to detect amplitude modulation with rate and temporal codes: neurometric analysis. J Neurophysiol 107:3325–3341.

Joris PX, Schreiner CE, Rees A (2004) Neural processing of amplitude-modulated sounds. Physiol Rev 84:541–577.

Jowa L, Howd R (2011) Should atrazine and related chlorotriazines be considered carcinogenic for human health risk assessment? J Environ Sci Health Part C Environ Carcinog Ecotoxicol Rev 29:91–144.

Juarez-Salinas DL, Engle JR, Navarro XO, Recanzone GH (2010) Hierarchical and serial processing in the spatial auditory cortical pathway is degraded by natural aging. J Neurosci 30:14795–14804.

Kelly JB, Cooke JE, Gilbride PC, Mitchell C, Zhang H (2006) Behavioral Limits of Auditory Temporal Resolution in the Rat: Amplitude Modulation and Duration Discrimination. J Comp Psychol 120:98–105.

Kurt S, Crook JM, Ohl FW, Scheich H, Schulze H (2006) Differential effects of iontophoretic in vivo application of the GABA(A)-antagonists bicuculline and gabazine in sensory cortex. Hear Res 212:224–235.

Lee HJ, Wallani T, Mendelson JR (2002) Temporal processing speed in the inferior colliculus of young and aged rats. Hear Res 174:64–74.

Lenaz G, Bovina C, D'aurelio M, Fato R, Formiggini G, Genova ML, Giuliano G, Pich MM, Paolucci U, Castelli GP, Ventura B (2002) Role of Mitochondria in Oxidative Stress and Aging. Ann N Y Acad Sci 959:199–213.

Levene H (1960) Robust Tests for Equality of Variances. In: Contributions to Probability and Statistics: Essays in Honor of Harold Hotelling, Stanford University Press., pp 278–292. Palo Alto: I. Olkin, et al.

Ling LL, Hughes LF, Caspary DM (2005) Age-related loss of the GABA synthetic enzyme glutamic acid decarboxylase in rat primary auditory cortex. Neuroscience 132:1103–1113.

Lix LM, Keselman JC, Keselman HJ (1996) Consequences of Assumption Violations Revisited: A Quantitative Review of Alternatives to the One-Way Analysis of Variance F Test. Rev Educ Res 66:579–619.

Lutman ME, Gatehouse S, Worthington AG (1991) Frequency resolution as a function of hearing threshold level and age. J Acoust Soc Am 89:320–328.

Lyon RF, Katsiamis AG, Drakakis EM (2010) History and future of auditory filter models. In: Proceedings of 2010 IEEE International Symposium on Circuits and Systems, pp 3809–3812.

Manunta Y, Edeline JM (1997) Effects of noradrenaline on frequency tuning of rat auditory cortex neurons. Eur J Neurosci 9:833–847.

Manunta Y, Edeline JM (1998) Effects of noradrenaline on rate-level function of auditory cortex neurons: is there a "gating" effect of noradrenaline? Exp Brain Res Exp Hirnforsch Expérimentation Cérébrale 118:361–372.

Manunta Y, Edeline J-M (2004) Noradrenergic induction of selective plasticity in the frequency tuning of auditory cortex neurons. J Neurophysiol 92:1445–1463.

Mattson MP, Liu D (2002) Energetics and oxidative stress in synaptic plasticity and neurodegenerative disorders. NeuroMolecular Med 2:215–231.

Mendelson JR, Lui B (2004) The effects of aging in the medial geniculate nucleus: a comparison with the inferior colliculus and auditory cortex. Hear Res 191:21–33.

Mendelson JR, Ricketts C (2001) Age-related temporal processing speed deterioration in auditory cortex. Hear Res 158:84–94.

Meyer AC, Frank T, Khimich D, Hoch G, Riedel D, Chapochnikov NM, Yarin YM, Harke B, Hell SW, Egner A, Moser T (2009) Tuning of synapse number, structure and function in the cochlea. Nat Neurosci 12:444–453.

Möhrle D, Ni K, Varakina K, Bing D, Lee SC, Zimmermann U, Knipper M, Rüttiger L (2016) Loss of auditory sensitivity from inner hair cell synaptopathy can be centrally compensated in the young but not old brain. Neurobiol Aging 44:173–184.

Moore BC, Peters RW, Glasberg BR (1992) Detection of temporal gaps in sinusoids by elderly subjects with and without hearing loss. J Acoust Soc Am 92:1923–1932.

Müller M (1991) Frequency representation in the rat cochlea. Hear Res 51:247–254.

Ng C-W, Navarro X, Engle JR, Recanzone GH (2015) Age-related changes of auditory brainstem responses in nonhuman primates. J Neurophysiol 114:455–467.

Noreña AJ, Eggermont JJ (2005) Enriched acoustic environment after noise trauma reduces hearing loss and prevents cortical map reorganization. J Neurosci 25:699–705.

Occelli F, Suied C, Pressnitzer D, Edeline J-M, Gourévitch B (2016) A Neural Substrate for Rapid Timbre Recognition? Neural and Behavioral Discrimination of Very Brief Acoustic Vowels. Cereb Cortex 26:2483–2496.

Ouda L, Burianova J, Syka J (2012) Age-related changes in calbindin and calretinin immunoreactivity in the central auditory system of the rat. Exp Gerontol 47:497–506.

Ouda L, Druga R, Syka J (2008) Changes in parvalbumin immunoreactivity with aging in the central auditory system of the rat. Exp Gerontol 43:782–789.

Ouellet L, de Villers-Sidani E (2014) Trajectory of the main GABAergic interneuron populations from early development to old age in the rat primary auditory cortex. Front Neuroanat 8:40.

Palombi PS, Caspary DM (1996a) Physiology of the aged Fischer 344 rat inferior colliculus: responses to contralateral monaural stimuli. J Neurophysiol 76:3114–3125.

Palombi PS, Caspary DM (1996b) Responses of young and aged Fischer 344 rat inferior colliculus neurons to binaural tonal stimuli. Hear Res 100:59–67.

Paraouty N, Lorenzi C (2017) Using individual differences to assess modulation-processing mechanisms and age effects. Hear Res 344:38–49.

Parham K, McKinnon BJ, Eibling D, Gates GA (2011) Challenges and Opportunities in Presbycusis. Otolaryngol Neck Surg 144:491–495.

Paxinos G, Watson C (2005) The Rat Brain in Stereotaxic Coordinates. Elsevier Academic Press.

Pearlman RC (1982) Presbycusis: the need for a clinical definition. Am J Otol 3:183–186.

Penney J, Tsai L-H (2014) Histone deacetylases in memory and cognition. Sci Signal 7:re12–re12.

Portfors CV (2007) Types and Functions of Ultrasonic Vocalizations in Laboratory Rats and Mice. J Am Assoc Lab Anim Sci 46:28–34.

Richardson BD, Ling LL, Uteshev VV, Caspary DM (2013) Reduced GABAA Receptor-Mediated Tonic Inhibition in Aged Rat Auditory Thalamus. J Neurosci 33:1218–1227.

Roger M, Arnault P (1989) Anatomical study of the connections of the primary auditory area in the rat. J Comp Neurol 287:339–356.

Sanz-Fernández R, Sánchez-Rodriguez C, Granizo JJ, Durio-Calero E, Martín-Sanz E (2015) Accuracy of auditory steady state and auditory brainstem responses to detect the preventive effect of polyphenols on age-related hearing loss in Sprague-Dawley rats. Eur Arch Oto-Rhino-Laryngol Off J Eur Fed Oto-Rhino-Laryngol Soc EUFOS Affil Ger Soc Oto-Rhino-Laryngol - Head Neck Surg.

Schmiedt RA, Mills JH, Boettcher FA (1996) Age-related loss of activity of auditory-nerve fibers. J Neurophysiol 76:2799–2803.

Schnupp JWH, Hall TM, Kokelaar RF, Ahmed B (2006) Plasticity of temporal pattern codes for vocalization stimuli in primary auditory cortex. J Neurosci Off J Soc Neurosci 26:4785–4795.

Schoof T, Rosen S (2014) The role of auditory and cognitive factors in understanding speech in noise by normal-hearing older listeners. Front Aging Neurosci 6 Available at: http://journal.frontiersin.org/article/10.3389/fnagi.2014.00307/full [Accessed May 17, 2017].

Schuknecht HF (1955) Presbycusis. The Laryngoscope 65:402–419.

Schuknecht HF, Kirchner JC (1974) Cochlear otosclerosis: Fact or fantasy. The Laryngoscope 84:766–782.

Sergeyenko Y, Lall K, Liberman MC, Kujawa SG (2013) Age-Related Cochlear Synaptopathy: An Early-Onset Contributor to Auditory Functional Decline. J Neurosci 33:13686–13694.

Sethi MK, Zaia J (2017) Extracellular matrix proteomics in schizophrenia and Alzheimer's disease. Anal Bioanal Chem 409:379–394.

Shetake JA, Wolf JT, Cheung RJ, Engineer CT, Ram SK, Kilgard MP (2011) Cortical activity patterns predict robust speech discrimination ability in noise. Eur J Neurosci 34:1823–1838.

Simon H, Frisina RD, Walton JP (2004) Age reduces response latency of mouse inferior colliculus neurons to AM sounds. J Acoust Soc Am 116:469–477.

Song I, Dityatev A (2017) Crosstalk between glia, extracellular matrix and neurons. Brain Res Bull Available at: http://www.sciencedirect.com/science/article/pii/S0361923017301351 [Accessed May 17, 2017].

Sottile SY, Ling L, Cox BC, Caspary DM (2017) Impact of ageing on postsynaptic neuronal nicotinic neurotransmission in auditory thalamus. J Physiol 595:5375–5385.

Stamataki S, Francis HW, Lehar M, May BJ, Ryugo DK (2006) Synaptic alterations at inner hair cells precede spiral ganglion cell loss in aging C57BL/6J mice. Hear Res 221:104–118.

Stenqvist M (2000) Age-related hearing changes and effects of exotoxin on inner ear function in aging rat. A frequency-specific auditory brainstem response study. ORL J Oto-Rhino-Laryngol Its Relat Spec 62:13–19.

Strough J, de Bruin WB, Peters E (2015) New perspectives for motivating better decisions in older adults. Front Psychol 6:783.

Tarnowski BI, Schmiedt RA, Hellstrom LI, Lee FS, Adams JC (1991) Age-related changes in cochleas of mongolian gerbils. Hear Res 54:123–134.

Tillein J, Hubka P, Kral A (2016) Monaural Congenital Deafness Affects Aural Dominance and Degrades Binaural Processing. Cereb Cortex 26:1762–1777.

Turner JG, Hughes LF, Caspary DM (2005) Affects of aging on receptive fields in rat primary auditory cortex layer V neurons. J Neurophysiol 94:2738–2747.

Turner JG, Willott JF (1998) Exposure to an augmented acoustic environment alters auditory function in hearing-impaired DBA/2J mice. Hear Res 118:101–113.

Verde ME, MacMillan NA, Rotello CM (2006) Measures of sensitivity based on a single hit rate and false alarm rate: the accuracy, precision, and robustness of d', Az, and A'. Percept Psychophys 68:643–654.

Villanueva-Castillo C, Tecuatl C, Herrera-López G, Galván EJ (2017) Aging-related impairments of hippocampal mossy fibers synapses on CA3 pyramidal cells. Neurobiol Aging 49:119–137.

Walton JP (2010) Timing is everything: temporal processing deficits in the aged auditory brainstem. Hear Res 264:63–69.

Walton JP, Frisina RD, Meierhans LR (1995) Sensorineural hearing loss alters recovery from short-term adaptation in the C57BL/6 mouse. Hear Res 88:19–26.

Walton JP, Simon H, Frisina RD (2002) Age-Related Alterations in the Neural Coding of Envelope Periodicities. J Neurophysiol 88:565–578.

Wang J, Caspary D, Salvi RJ (2000) GABA-A antagonist causes dramatic expansion of tuning in primary auditory cortex. Neuroreport 11:1137–1140.

Williamson TT, Zhu X, Walton JP, Frisina RD (2015) Auditory brainstem gap responses start to decline in mice in middle age: a novel physiological biomarker for age-related hearing loss. Cell Tissue Res 361:359–369.

Willott JF, Parham K, Hunter KP (1988) Response properties of inferior colliculus neurons in young and very old CBA/J mice. Hear Res 37:1–14.

Willott JF, Turner JG (1999) Prolonged exposure to an augmented acoustic environment ameliorates age-related auditory changes in C57BL/6J and DBA/2J mice. Hear Res 135:78–88.

Willott JF, Turner JG, Sundin VS (2000) Effects of exposure to an augmented acoustic environment on auditory function in mice: roles of hearing loss and age during treatment. Hear Res 142:79–88.

Figure Legends

Figure 1: Example of CAP, ABR and cortical thresholds for a 15-month-old rat (#261).

CAP (A) and ABR (B) recordings in response to a short pure tone of 8 kHz for sound pressure levels (SPL) of 0 to 80dB. The response amplitude is quantified by the N1-P1 amplitude difference for CAP and by the wave II amplitude for ABRs. C. In the cortex, the maximum firing rate of a cortical site is shown in response to tones varying in frequency (abcissa) and SPL (ordinate). The dashed line is the contour at 6 SD above spontaneous activity and determines the threshold of the cortical site. D. Each cortical site sampled on this animal generated a threshold tuning curve (blue lines) and the pink line indicates the lowest cortical thresholds as a function of frequency. Note that, except at 16 kHz, there is a good match between ABR and the lowest cortical threshold. E. Simplified cheme summarizing the different stages of auditory pathways at which recordings were acquired.

Figure 2: In the cochlea, DPOAEs and synaptic ribbons are normal in old animals

A. Amplitude of DPOAEs as a function of frequency for animals aged 9, 15 and 21 months, with the gray line indicating the noise level.

B. Simultaneous labeling of presynaptic inner hair cell (IHC) ribbons with a mouse anti-CtBP2 antibody (green) and of postsynaptic glutamate receptors (GluA2 subunit, red). The three lower panels show a magnification of labeling at the synaptic level.

C. Number of synapses per IHC as a function of the position of the ribbon synapse along the cochlea (abscissa). The frequencies corresponding to cochlear locations are indicated on the top axis (red). Each dot represents the average over 6 consecutive IHCs (Bourien et al., 2014). Solid curves are second-order polynomial fits (9 months, $f(x) = -0.005x^2+0.466x+8.9$, $r^2 > 0.9$; 21 months, $f(x) = -0.0054x^2+0.5x+8.7$, $r^2 > 0.9$, with x the position from the apex in percent).

Figure 3: Aging has deleterious effects on ABRs, but not CAPs.

Mean values of CAP thresholds (A), N1-P1 amplitude (B) and N1 latency (C) as a function of frequency for the different ages. B-C, E-F: for amplitude and latencies for both CAP and ABRs, the curves at 80 dB SPL, 60 dB SPL and 40 dB SPL are displayed on the same plot (CAP) or on three different plots (ABRs). Otherwise, D-F are similar to A-C for ABR thresholds, wave II amplitude and wave II latency, respectively. Gi, Gii Individual CAP (Gi) and ABR (Gii) at a frequency of 8 kHz and for two animals of aged 9 and 21 months, respectively, illustrating the unexpected lack of increase in latency with aging.

Figure 4. Cortex: the response to pure tones

A. Mean cortical thresholds as a function of frequency for the different ages.

B. Example of a spectrotemporal receptive field (STRF) obtained for a 21-month-old animal. The STRF shows the mean firing rate (color scale) obtained at a cortical site in response to pure tones (frequency, ordinate) and as a function of the time after tone onset (abscissa). Significant peaks (6 SD above spontaneous activity) are shown as a white contour.

C-G. The mean values of parameters extracted from STRFs (duration, bandwidth and first spike latency) are presented for three ranges of best frequency (the best frequency was defined as the frequency eliciting the maximum firing rate for the cortical site). The first spike latency (C), duration (D), bandwidth (E), maximum firing rate over baseline activity (F) and Q_{20dB} coefficient (G) are plotted as a function of animal age (abscissa) and for three ranges of best frequencies (low frequencies, LF: <8 kHz; mid-range frequencies, MF: 8-20 kHz; high frequencies, HF: >20 kHz).

Figure 5. Cortex: response to communication sounds

A. Examples of cortical responses to a guinea pig whistle (left) and a bird song (right). The temporal envelopes of sounds are represented on the top and the raster plots below present the neuronal responses for 25 presentations of each vocalization (at 75 dB SPL) without noise (0 dB) and with three levels of background noise (60 dB, 65 dB, 70 dB). The responses to the 25 trials are aligned vertically, with each line corresponding to one presentation. The values of the *CorrCoeff* index (quantifying the temporal reliability of neuronal response across trials) are indicated to the right of the neuronal responses.

B. Mean values of *CorrCoef* as a function of age for the responses to a guinea pig whistle for the 3 groups of best frequencies defined in Figure 4, in absence of noise (left) or with noise at 60 dB SPL or 70 dB SPL (center and right, respectively).

C. As for B, for the responses to birdsong.

Figure 6: Cortex: gap detection

A. Example of cortical responses to a guinea pig whistle including gaps of various durations. The temporal envelope of the guinea pig whistle is represented at the top, with a gap symbolized by a green rectangle. The peri-stimulus time histograms (PSTHs) displayed below correspond to neuronal responses to whistles with gaps ranging from 2 ms (bottom) to 64 ms (top). Each stimulus was presented 25 times. A red star indicates the observation of a significant peak in the PSTH within 50 ms of the gap.

B. Percentage of neurons responding to the presence of the gap as a function of gap duration (abcissa) for the three ages considered (colored lines).

C. Percentage of neurons responding to the presence of a 2 ms gap as a function of age (colored lines), for the 3 groups of best frequencies defined in Figure 4 (low, mid-range and high frequencies).

D. As for C, but for a gap of 8 ms.

E. As for C, but for a gap of 32 ms.

Figure 7: Cortex: temporal envelope

A-B. Examples of cortical responses to amplitude-modulated noise with a range of modulation rates between 2 Hz and 50 Hz, and a modulation depth of 100% (A), a modulation rate of 4 Hz and a range of modulation depths between 0 and 100% (B). The temporal envelope of an amplitude-modulated noise is represented at the top. For both types of stimuli, the peri-stimulus time histograms (PSTH) of neuronal responses are presented for 20 presentations of each stimulus. On the left of the PSTHs, the vector strength (VS) value (abscissa) is plotted as a function of modulation rate (left) or modulation depth (right).

C. Group data for the VS values for the temporal modulation transfer function (tMTF).

D. Averaged VS values for two sets of modulation rates (8-14 Hz, left; 20-32 Hz, right) as a function of animal age (colored lines) and for the 3 groups of best frequencies defined in Figure 4 (low, mid-range and high frequencies).

E-F. As for C and D, respectively, for modulation depth rather than modulation rate.

Figure 8: Cortex: Multidimensional analysis

A. Standard deviation (SD) of each parameter, split according to animal age. The parameters are those described in Figures 4-7, sometimes averaged across a subset of parameter values. For instance, Gaps (2-8) corresponds to the percentage of neurons detecting the presence of the gap for gap durations between 2 and 8 ms. SD values displayed here are across individuals of each age, normalized by the SD of each parameter with data pooled across all animals. The dashed horizontal lines are confidence intervals for SD values across all parameters at each age. Circled dots are those outside the confidence interval for each age.

B. Interanimal variability calculated as the variance across animals of all parameters, after the standardization of each parameter.

C-E. Principal component analysis of the parameter values. C. Inertia (variance) of the principal components. D. Age effect on each principal component: log-pvalue of ANOVA one-way test. E. Projections of values and the parameters of the principal components 2 and 4. Each point is associated with a cortical site. Each parameter is represented as a vector with a projected length on a given axis proportional to the correlation of this parameter with the axis. The centers ("+" signs) and the borders indicating the SD (colored circles) for the points associated with each group of animals age are superimposed in color.

Figure 9: GAD67 labeling of neurons in the primary auditory cortex

A. Example of immunostaining for GAD67 in the primary auditory cortex (40 x magnification; scale bar: 50 µm).

B. Density of GAD67-positive cells in the auditory cortex as a function of animal age (abscissa). Quantification was performed in the supragranular (II-III, labeled Sup) and infragranular (V-VI, labeled Deep) layers.

Figure 10: Modulation depth discrimination task

A. The behavioral task was an aversive Go-NoGo protocol in a shuttle box. The animal should discriminate between noise with (SC+, Go) and without (SC-, NoGo) amplitude modulation at 4 Hz, the level of depth modulation varying between 20 and 100%. For details, see methods.

B. Performance of animals as a function of age (colored lines). The percentage of animals achieving correct discrimination is represented as a function of the smallest depth modulation

that the animals can discriminate from non-modulated white noise. The percentage of animals failing to achieve the criteria for correct discrimination is indicated on the left.

C. Latency of motor responses to CS+ presentations, as a function of animal age (abscissa). This latency was the time interval between the onset of the tone and the movement of the animal into the other compartment. We recorded the 10 shortest latencies per animal in response to CS+ stimuli when the animals had mastered the discrimination between the constant white noise and the 100% depth of amplitude modulation (after 3 successful sessions).

Table 1: Number of animals of the different ages used

Age	Behavior	AI	CAP/ABRs (free field)	DPOAEs	Immunochemistry
9 months	*n*=10	9	7	8	4
15 months	*n*=9	8	8	9	6
21 months	*n*=12 [a]	8	5	5	5

[a] Four 21-month-old animals were used in the behavioral task but died before the electrophysiological recording session (at the beginning or in the middle of surgery).

Table 2: Number of cortical sites recorded for the different groups of age as a function of the Best Frequency (BF) value.

Age	Low frequency (BF<8 kHz)	Medium frequency (8<BF<20kHz)	High frequency (BF<8 kHz)
6 months	125	142	169
9 months	102	131	193
15 months	126	91	157
21 months	90	216	92

Figure1

Click here to download high resolution image

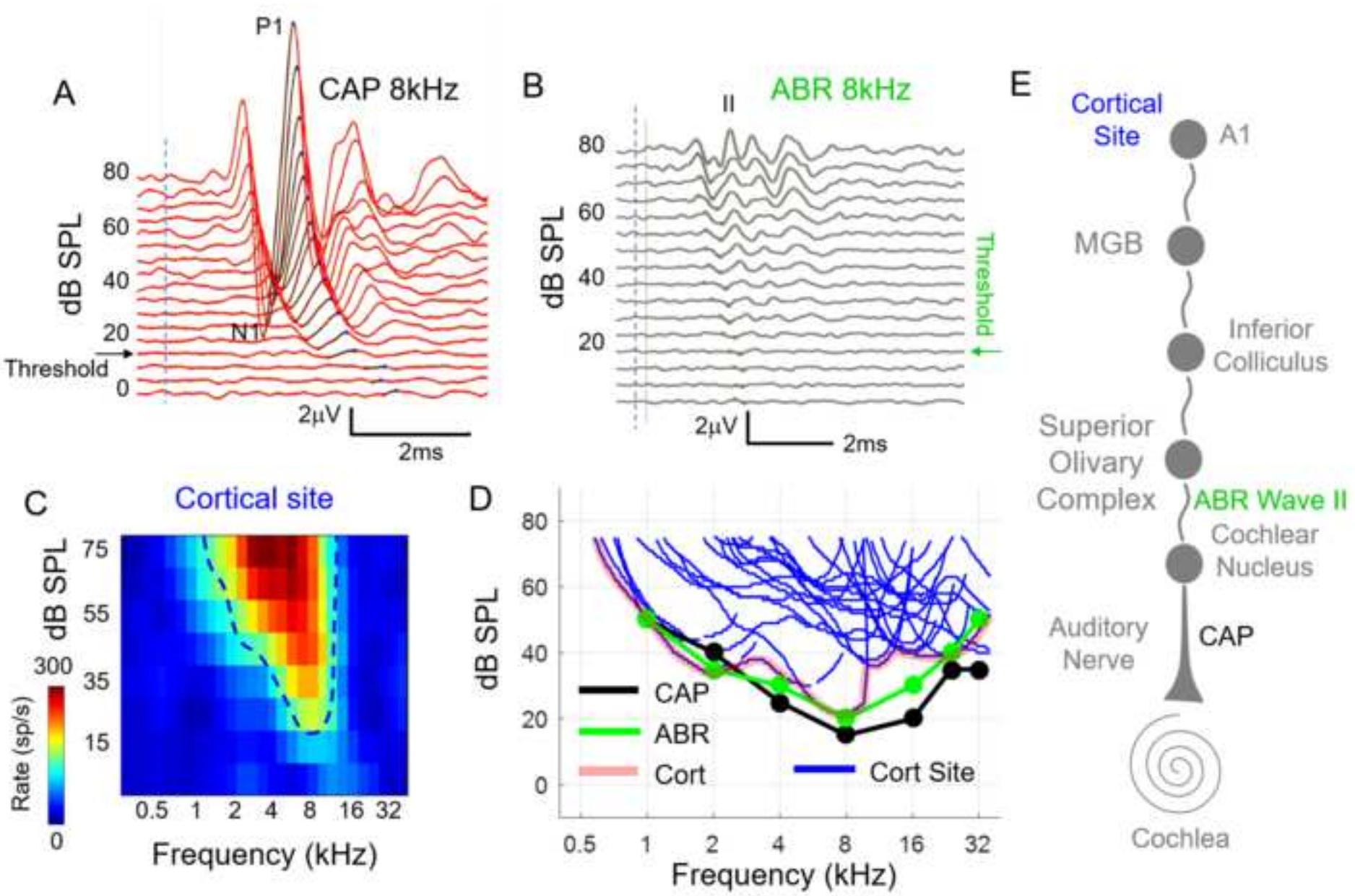

Figure2

Click here to download high resolution image

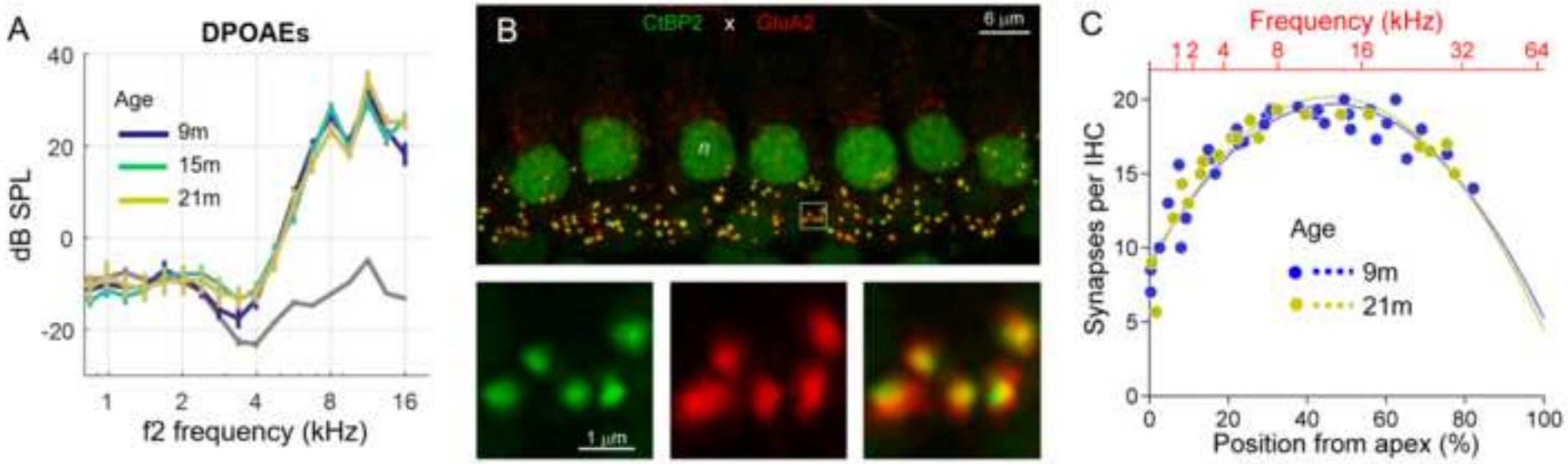

Figure3

Click here to download high resolution image

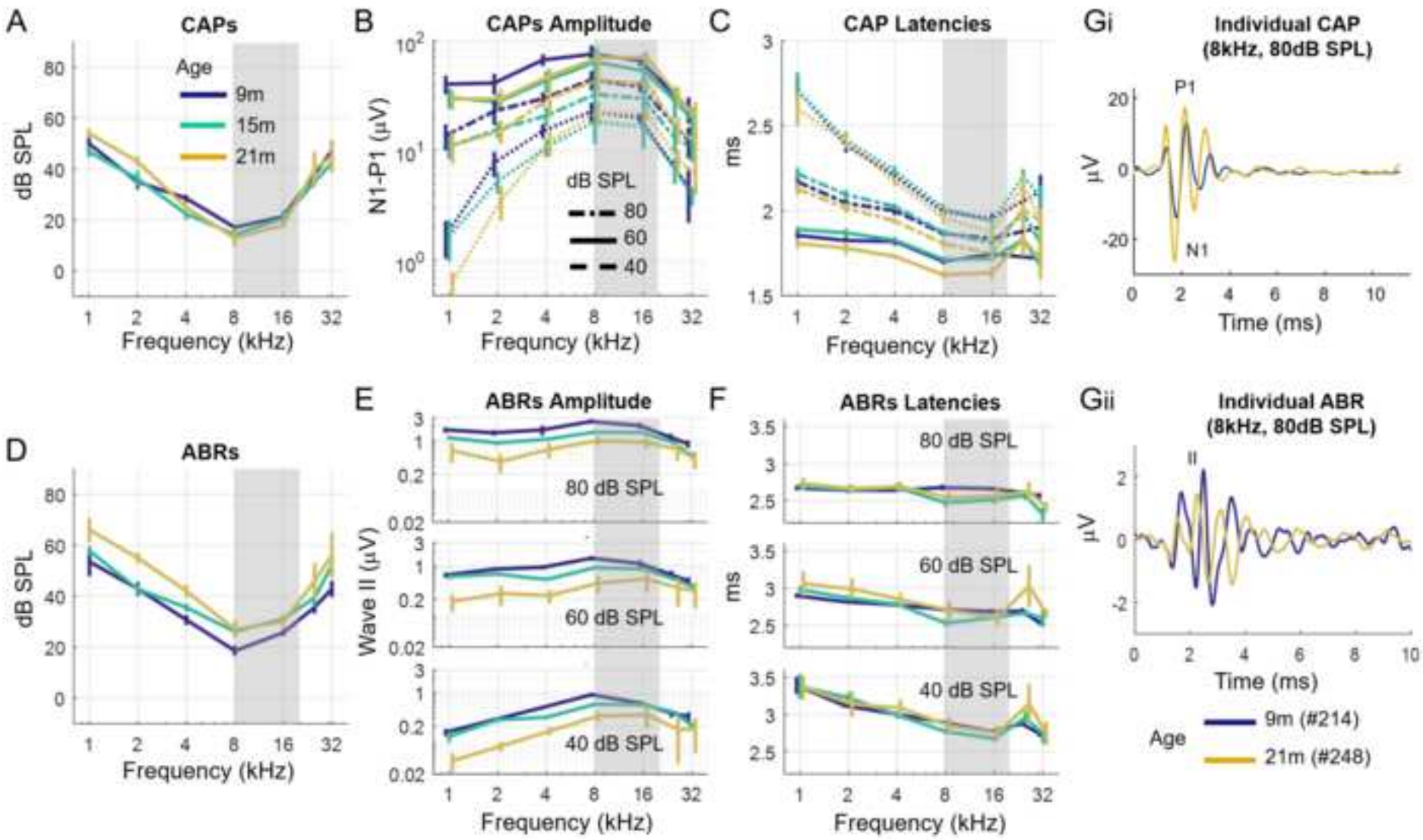

Figure4

Click here to download high resolution image

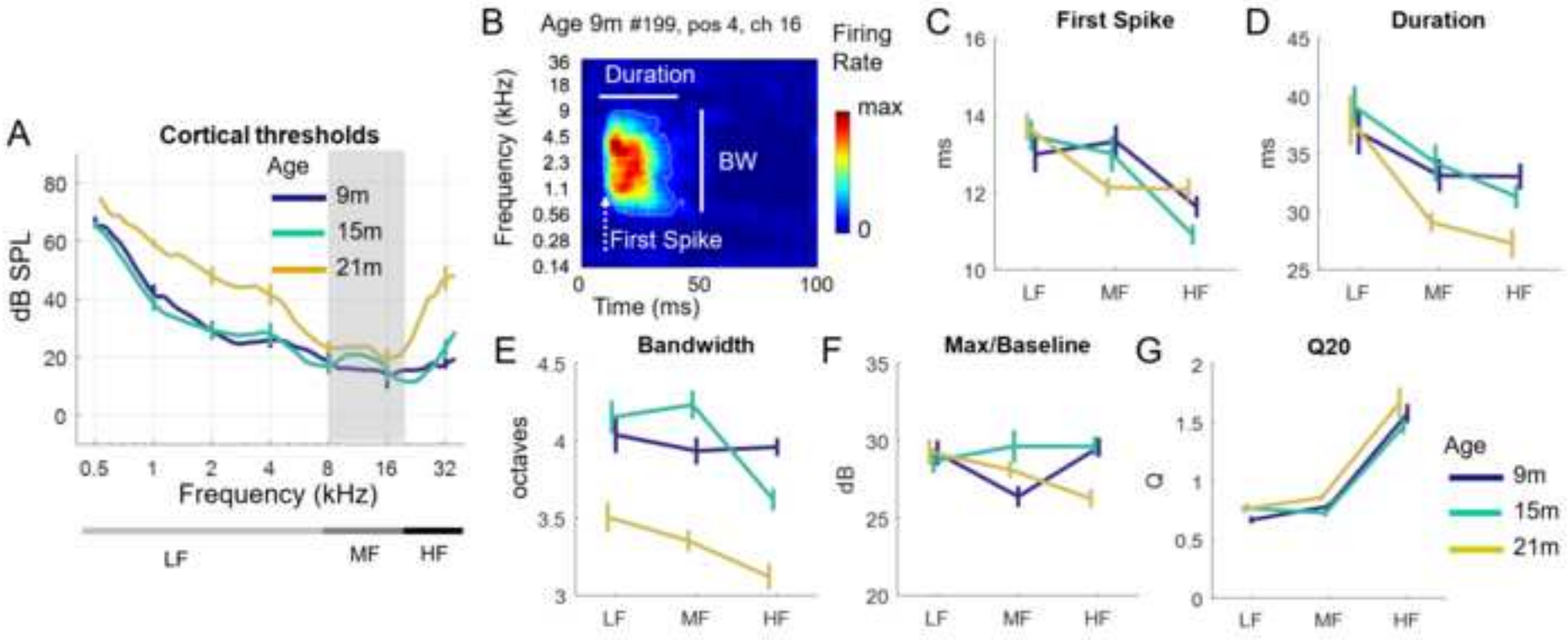

Figure5
Click here to download high resolution image

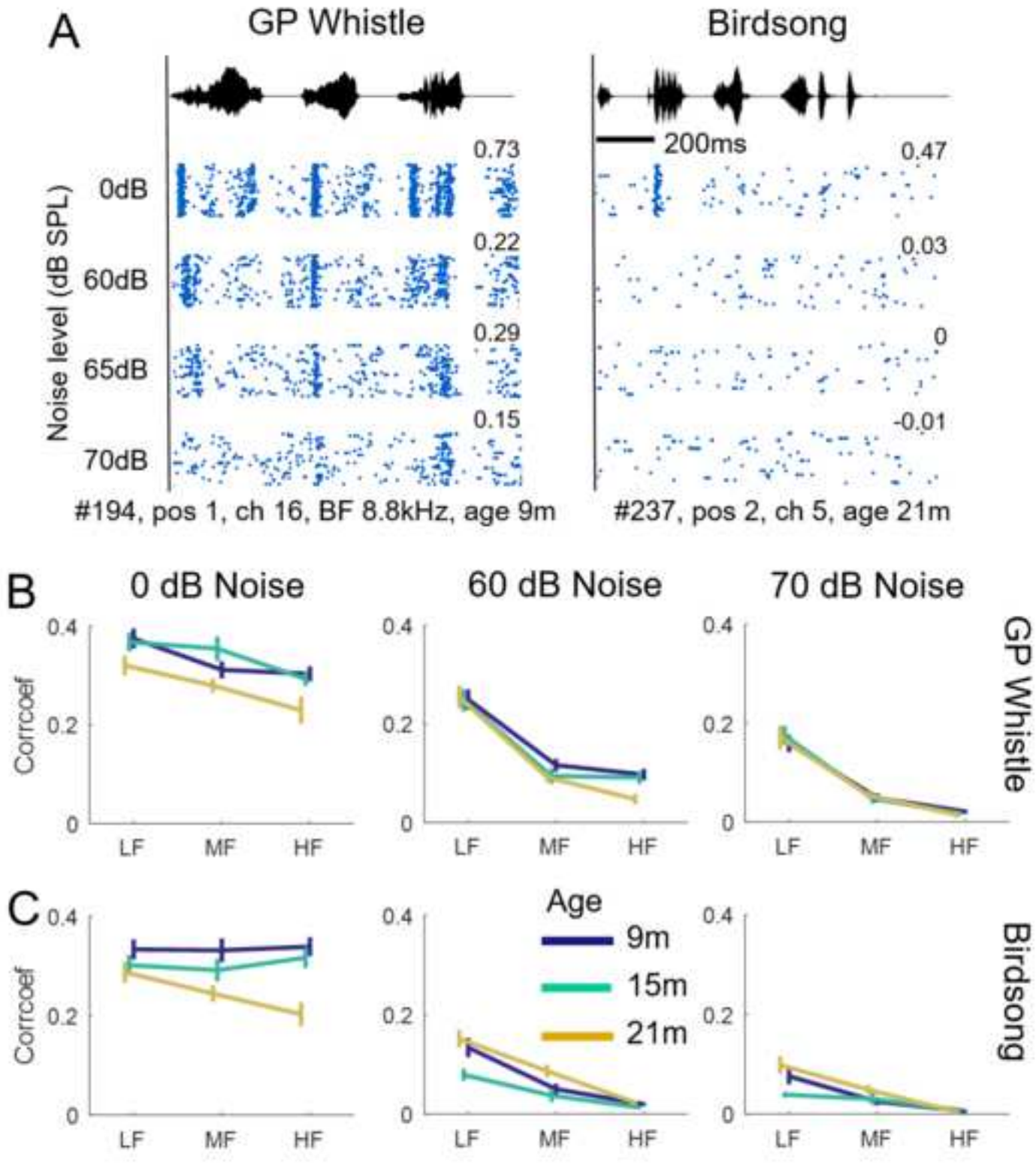

Figure6

Click here to download high resolution image

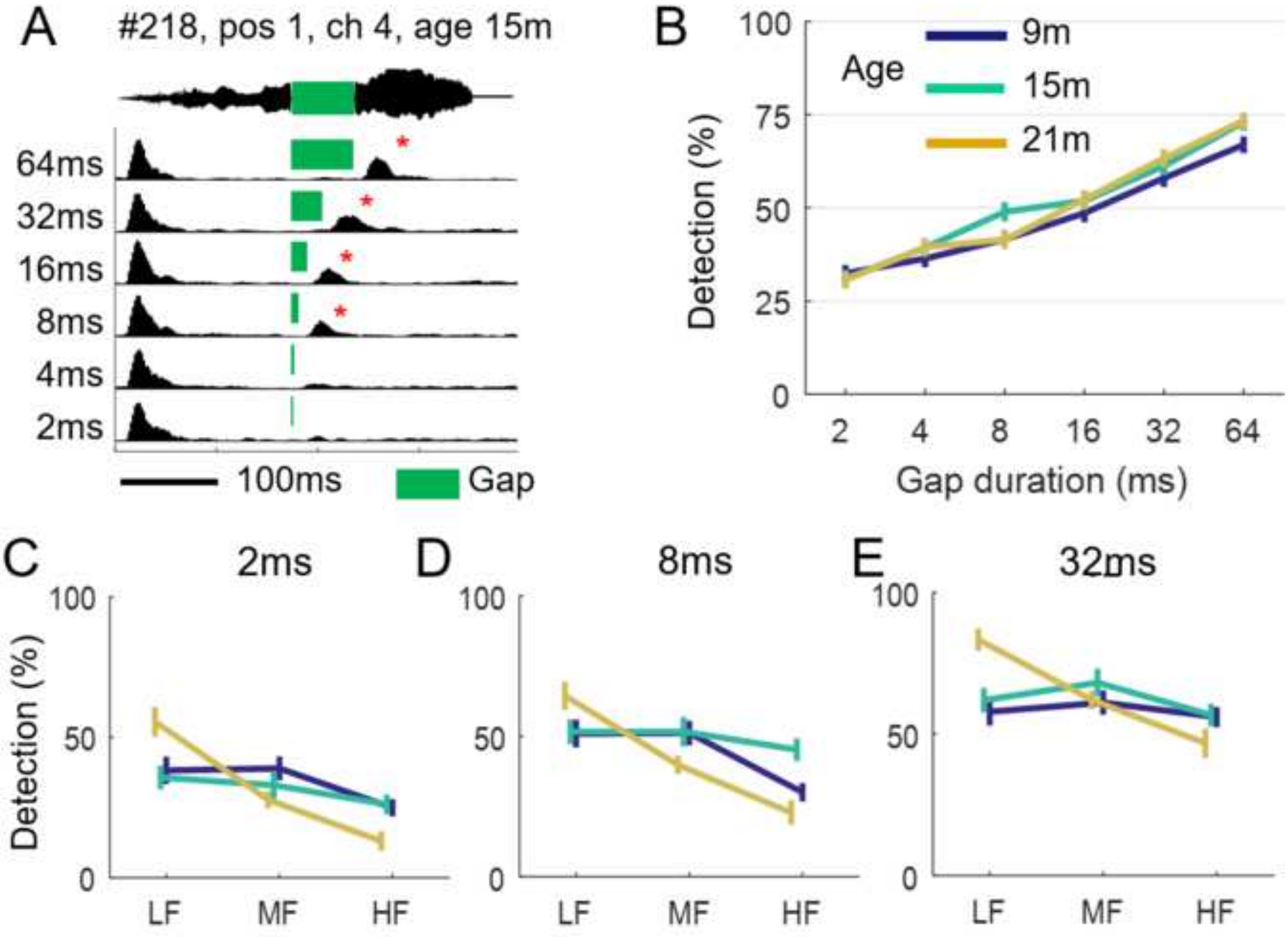

Figure7

Click here to download high resolution image

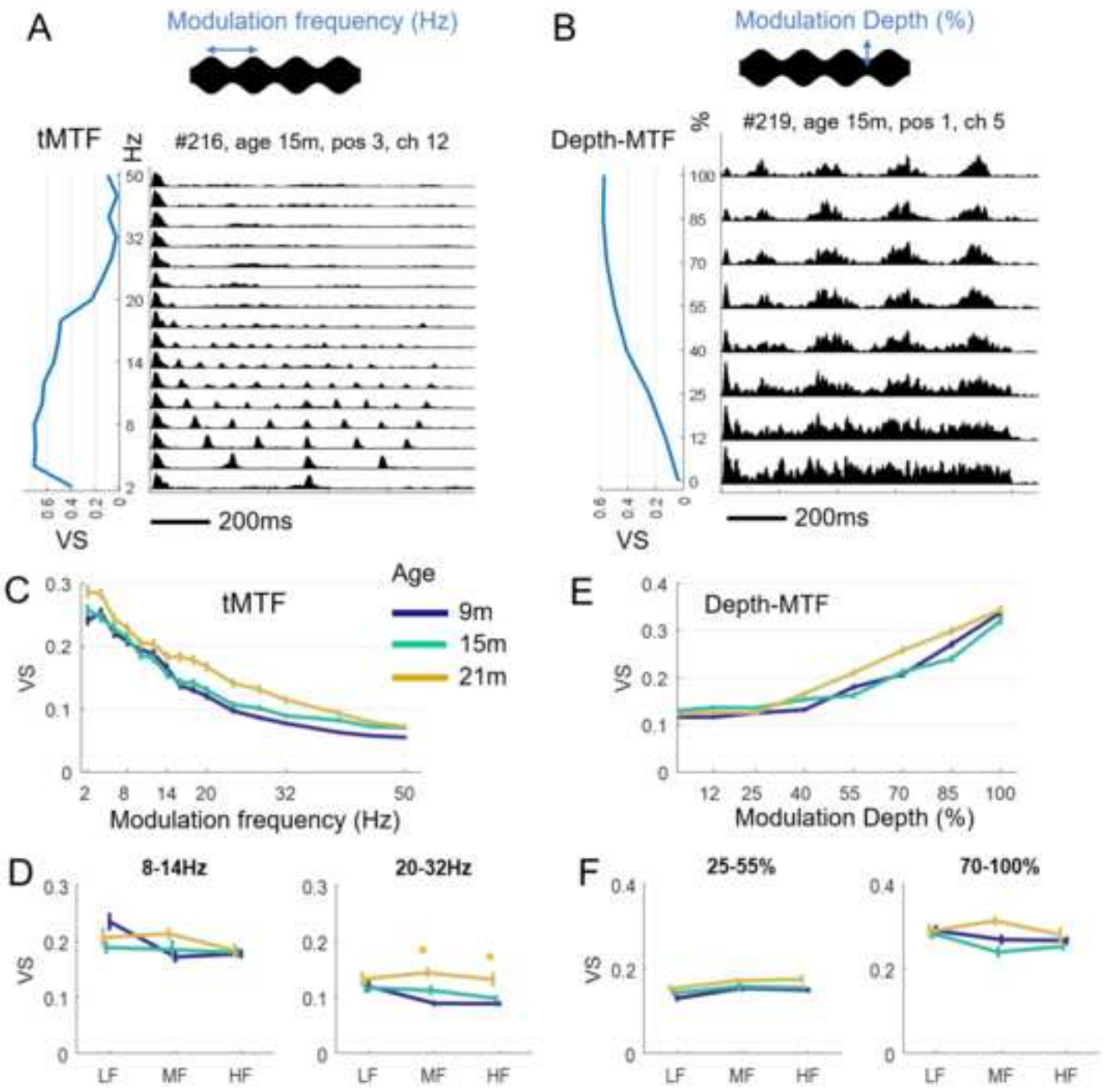

Figure8

Click here to download high resolution image

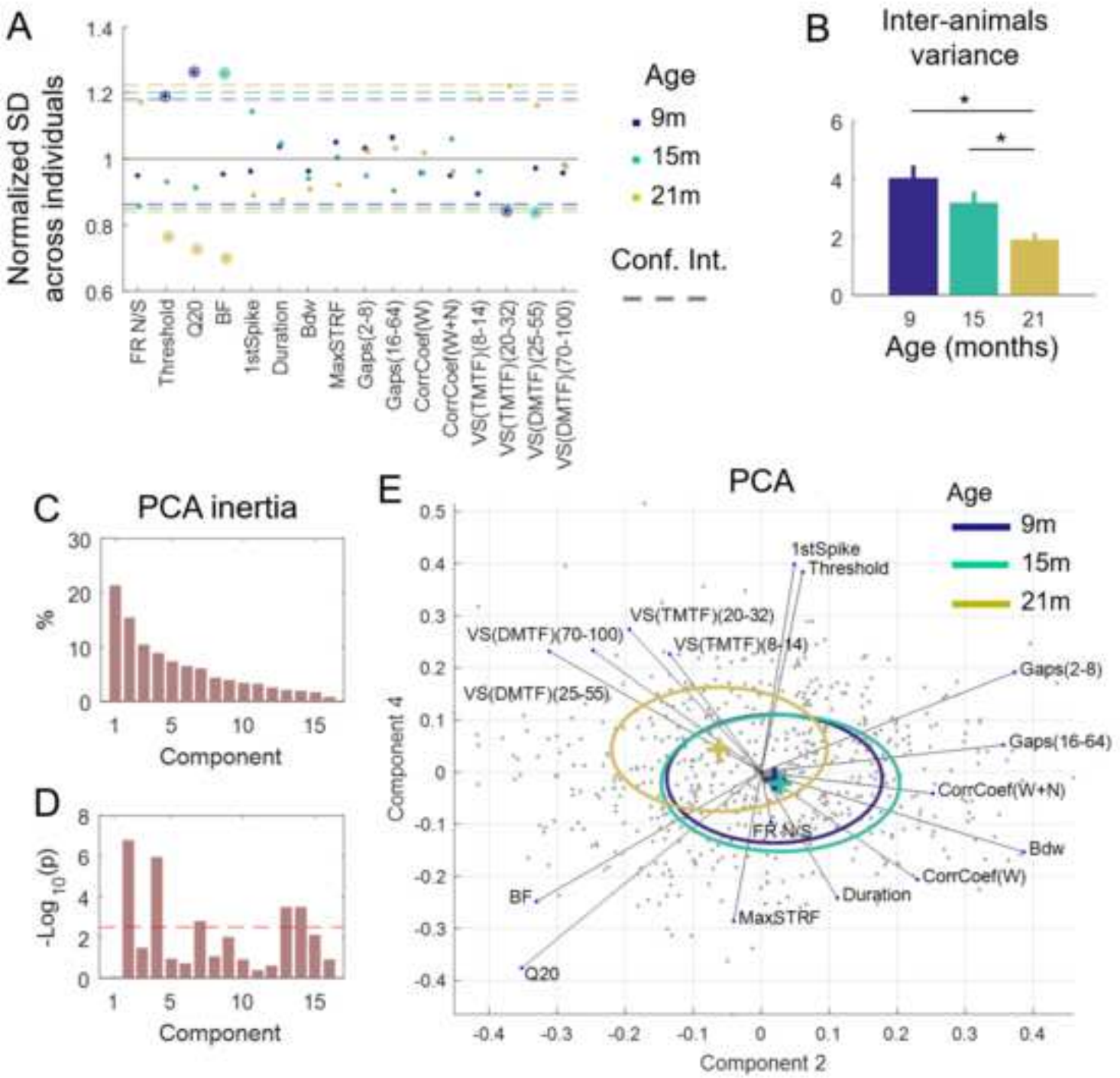

Figure9
Click here to download high resolution image

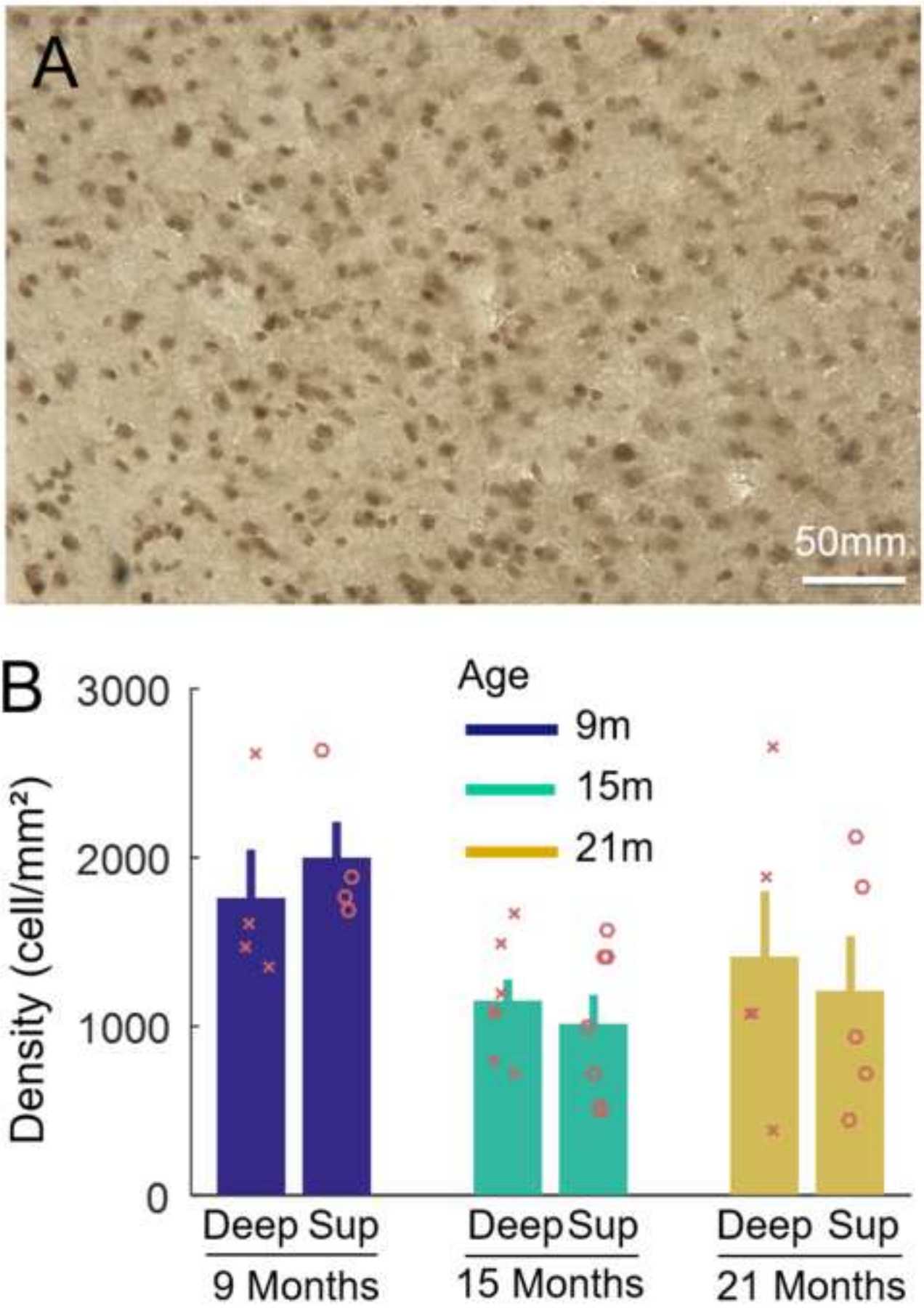

Figure10

Click here to download high resolution image